



# **Cell-Free Biocatalytic Modules Mediated by a Solid-Binding Peptide**

**By Emily Seu Yin Gibson**

**BMedSci**

**Department of Chemistry and Biomolecular Sciences**

**Macquarie University**

**Submitted for examination on October 9<sup>th</sup>, 2015**

A thesis

submitted in partial fulfilment

to the requirements for the degree

of

**Master of Research**



Solid-binding peptides (SBPs) are short peptide sequences that selectively recognise and bind to solid support materials. They can act as molecular Linkers to direct the orientated immobilisation of proteins and enzymes onto solid materials without compromising their biological function. SBPs have been used mostly as molecular tools for functionalisation of nanomaterials. However, little is known about the potential use of SBPs for the immobilisation of enzymes and their application in industrial-scale biocatalysis. The SBP used in this project displays strong and selective binding affinity to silica-based materials like silica and zeolite. These are considered ideal supports for enzyme immobilisation in industrial processes as they offer unique properties including high mechanical strength and stability, are chemically inert and can be used over a wide range of operating pressures and conditions.

This project aims to explore the potential of combining SBPs, inexpensive silica-based matrices and polysaccharide-degrading enzymes into functional biocatalytic modules for potential industrial applications. This will be a proof of concept project designed to investigate the effect of incorporating the SBP into thermophilic enzymes and establish the minimum requirement to set up functional cell-free biocatalytic modules. Biocatalytic modules containing multiple thermophilic enzymes retain function under conditions suitable for large-scale industrial biocatalysis.

**Statement of Candidate**

This is to certify that the research contained in this thesis titled 'Cell-Free Biocatalytic Modules Mediated by a Solid-Binding Peptide' is my own work. This thesis has not been submitted to any institutions other than Macquarie University for any degree or other purposes. I certify that the intellectual content of this thesis is the product of my own work and that all assistance received in preparing this thesis and sources have been appropriately acknowledged and referenced.

Furthermore, biosafety approval for the work carried out in this thesis was appropriately obtained and filed under: Exempt Dealing, "Incorporation of a linker peptide to industrially-relevant enzymes" (Ref. No: 5201500124).

Emily Seu Yin Gibson (42441331)

## **Acknowledgements**

First and foremost, to my supervisor, Dr. Anwar Sunna. Thank you for your endless vision, patience and assistance in guiding me through this thesis. This thesis wouldn't have been possible without your dedication and enthusiasm.

Next, to Professor Peter Bergquist, for his tireless editing, suggestions and improvements on this thesis. Your turnaround time is incredible and a little bit scary.

Next, to my officemates: Andrew, Alex, Kerstin, Vinoth, and Sameera, for being excellent lunch and coffee buddies, as well as sounding boards and advice-givers.

Next, to my fellow MRes students Mike, Ben, and Dom, for the support, listening, laughs, and commiserating.

Next, to my family, for their endless support in the face of economics, statistics, engineering, and computer science backgrounds. Even though I was once asked if proteins are minerals, your support means the world to me.

And finally, to Brent, for keeping me sane, for the Wednesday night dinners, for dragging me back to the real world when I needed it, and for getting me hooked on Game of Thrones at the worst possible time.

I also wish to acknowledge Nicole Vella and Nadia Suarez-Bosche from the Microscopy Unit, Faculty of Science and Engineering, Macquarie University, for their assistance with scanning electron microscopy and sample preparation.

# Contents

Chapter 1 Introduction .....	1
Enzyme Immobilisation .....	1
Solid Binding Peptides as a New Immobilisation Tool.....	7
The project.....	16
Chapter 2 Materials and Methods.....	21
Chapter 3 Results.....	27
Chapter 4 Discussion .....	47
Chapter 5 References .....	54
Chapter 6 Supplementary material .....	59

# **Cell-Free Biocatalytic Modules Mediated by a Solid-Binding Peptide**

## **Chapter 1 Introduction**

### **Enzyme Immobilisation**

Enzymes are important tools in the production of useful industrial biotechnological products. Immobilised enzymes fixed to a solid support allow for cell-free production of industrially-important products. Enzyme immobilisation has many applications in biotechnology and an emerging use of enzyme immobilisation is for the creation of cell-free biocatalytic pathways for production at an industrial scale.

Enzyme immobilisation aims to attach enzymes to a solid support material while retaining comparable or better activity than the free enzyme. Immobilised enzymes have a number of advantages over free enzymes, especially in an industrial setting. Due to the presence of an inorganic support, the immobilised enzymes are insoluble in the reaction medium, meaning they can be removed easily to prevent end product contamination [1]. Removal of the enzymes also facilitates reuse in multiple subsequent reactions, reducing production costs [2]. If end product inhibition occurs, more immobilised enzyme can be added easily to the reaction to overcome this problem as well as the addition of subsequent enzymes in a pathway [3].

A good immobilisation technique should favour the protein-support reaction over undesired side reactions or protein-protein interactions. Critical variables include reaction time, which must be of a sufficient length to allow for alignment of the enzyme and the support; pH, which can affect the binding ability and the activity of the enzyme; and temperature as extremes can induce conformational changes in enzymes [4]. The immobilisation procedure may affect the activity of the enzyme, and cosolvents or other protein stabilisers such as glycerol may need to be added to the immobilisation buffer [5]. Buffers chosen should not interfere with the immobilisation reaction. For

example, certain amino compounds (e.g. Tris or 2-aminoethanol) may modify epoxy supports, or compete for key immobilisation residues and have marked temperature coefficients [4].

## **Conventional enzyme immobilisation techniques**

### *Non-specific adsorption*

Non-specific adsorption relies on the natural affinity certain protein domains have for inorganic materials [6]. They bind in a non-specific manner to the inorganic support through hydrogen bonding, van der Waals forces and ionic hydrophobic interactions. No chemical reaction is necessary. However, the adsorption is random, resulting in a proportion of active sites facing towards the support rather than the reaction medium [6]. This phenomenon may lead to a reduction in specific activity compared to the free enzyme. The interactions are the weakest of the enzyme immobilisation procedures, resulting in enzyme leaching off the support and into the reaction medium. This aspect is detrimental if the immobilised enzyme experiences sub-optimal conditions (like unexpected fluctuations in pH or temperature), as well as for long-term stability and enzyme reuse.

### *Covalent modification*

Covalent modification involves chemical modification of the enzyme to facilitate the formation of covalent bonds between the enzyme and the inorganic support material. This procedure usually involves functionalising the inorganic support with appropriate reactive groups [7]. Covalently immobilised enzymes are bound strongly to the support through the covalent bonds, and are not in danger of enzyme leaching off the support [2]. However, covalent modification involves chemical agents that may affect residues at the active site of the protein, leading to a reduction in biological activity [7]. The modification process may contain many different steps and reagents, which is not ideal for an industrial setting where cost and simplicity are paramount [7].

Amino group coupling can be used to conjugate the amino group of a lysine residue or the N-terminal amino group of the enzyme to the support [8]. Several different reagents (e.g. cyanogen



bromide [9], aldehydes [10], azlactones [11], and carbonyl diimidazole [12]) and activated supports can be utilised to immobilise the enzyme via the available amino groups (Figure 1-1).

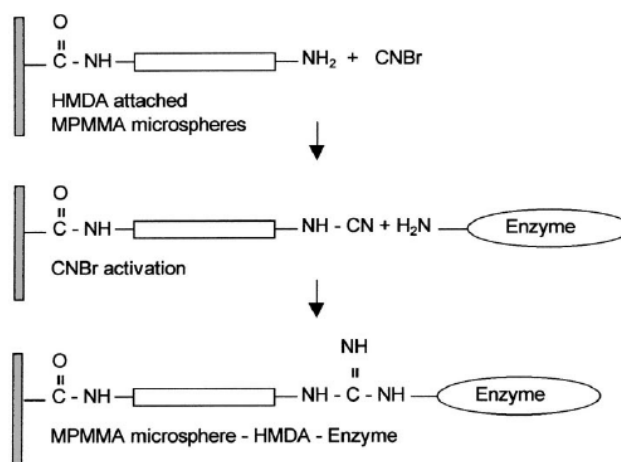


Figure 1-1: Cyanogen bromide immobilisation, an example of covalent modification through free amino-containing sidechains [9]. HMDA; hexamethylene diamine, MPMMA; magnetic poly(methylmethacrylate).

Using carboxyl groups for covalent immobilisation is best done with proteins containing a high percentage of aspartic acid or glutamic acid, which contain free carboxyl groups on their side chains [13]. They usually make up a large portion of surface groups in many proteins so that only mild coupling techniques are necessary [13]. EDC (N-(3-dimethylaminopropyl)-N'-ethylcarbodiimide) [14] and hydrazide [15] have been used for immobilisation via enzyme carbonyl or carboxyl groups.

Covalent modification can be done through thiol (S-H) groups located on cysteine side chains. Maleimides [16], iodoacetyl compounds [17], and pyridyl disulfide [18] have been used to immobilise enzymes via thiol groups using thioether linkages or disulfide exchanges. Cysteine thiols are often linked by cysteine-cysteine disulfide bridges so that only free cysteine side chains are available for coupling. This fact makes thiol group coupling much more selective than amino or carboxyl group coupling and cross-linking is less likely to affect structure as all of the structurally important cysteine residues are already present as disulfide bridges.

The immobilisation of multisubunit enzymes presents a series of unique challenges due to the risk of subunit dissociation that is not present with single-subunit enzymes. Multi-point covalent attachment uses multiple covalent reactions between the enzyme and a highly activated support in

order to immobilise a large multisubunit enzyme. All distances between the enzyme and the support must be carefully controlled to prevent unintentional conformational changes [19].

### *Encapsulation*

Encapsulated enzymes are enclosed in semipermeable membranes such as liposomes, biopolymers or microemulsion droplets [20]. This system protects the enzymes from any host proteases or unexpected changes in the reaction environment that may affect their activity, such as pH or temperature. However, encapsulating the enzymes often results in poor transfer of the substrate from the reaction medium to the active site of the enzyme [21]. Encapsulation started as a method optimised for chemically stable molecules and was not suited for enzymes which are much more unstable and prone to loss of function [22]. An improved method of encapsulation uses stabilised artificial liposomes that have been modified by adding hydrophobic monomers which interact with the hydrophobic core of the membrane [22]. These hydrophobic monomers, such as methacrylate, can be cross-linked to each other to stabilise the membrane [23]. To perform the encapsulation, the phospholipid membrane in a chloroform solution is dried under vacuum, and then rehydrated in a solution containing the enzyme [22].

Biomineralisation is a natural process where certain organisms use protein scaffolds to generate hard composite materials such as bones, shells, or teeth. This natural phenomenon has been used to encapsulate enzymes within biosilica nanoparticles using a silica-precipitating peptide and silicate precursor materials [1]. Silica-precipitating peptide R5 is a *Cylindrotheca fusiformis* silaffin protein found in the organism's silica skeleton. R5 has been used to create silica nanospheres 500nm in diameter that entraps the peptide and any other material in the reaction mixtures [1]. A range of materials have been successfully encapsulated, from enzymes to non-biological materials such as iron oxide nanoparticles, quantum dots, and iron oxide nanoparticles [1].

### *Entrapment*

Enzyme entrapment (Figure 1-2) works in a similar way to encapsulation, in that the enzymes are protected from direct contact with the reaction environment. Entrapment is achieved using a co-polymer network where one polymer is hydrophilic and one polymer is hydrophobic. The enzyme is loaded under aqueous conditions, where the hydrophilic polymer network swells and allows enzyme

uptake [3]. By placing the swollen network into an organic medium like *n*-heptane, the hydrophilic network shrinks and the hydrophobic network expands, trapping the enzyme. Poly(2-hydroxyethyl acrylate) has been used in a co-polymer network as the hydrophilic polymer with poly(dimethylsiloxane) as the hydrophobic polymer [24]. However, like encapsulation, entrapment suffers from poor substrate transfer between the enzyme and the reaction medium.

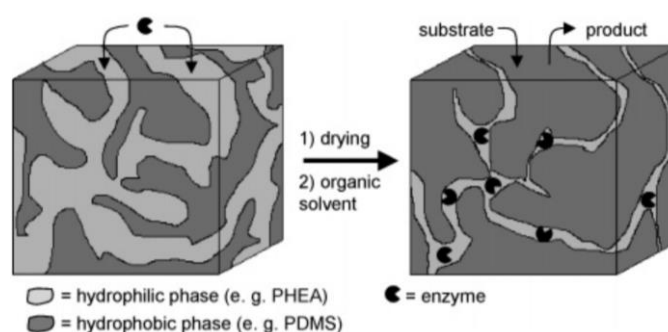


Figure 1-2: Enzyme entrapment in an amphiphilic network consisting of hydrophilic poly(2-hydroxyethyl acrylate) (PHEA) and hydrophobic poly(dimethylsiloxane) (PDMS) [24].

### *Cross-linked enzyme aggregates and crystals*

Cross-linking reactions involve covalently linking the enzymes to each other and there are two main methods. Cross-linked enzyme crystals (CLECs) are created by aggregating the enzymes through crystallisation. Microcrystals (approximately 0.1mm in size) are grown and cross-linked using a suitable reagent (such as glutaraldehyde) [25]. Crystals of this size are ideal for cross-linking because their surface area to volume ratio minimises substrate-product diffusion problems [25]. Using crystals as aggregates provides a naturally highly ordered structure and cross-linking the aggregates together prevents denaturation intermediates from forming [25]. Cross-linking based on the highly ordered structure of enzyme crystals helps to maintain activity of the enzymes. However, the crystallisation process can be lengthy, and requires enzymes of high purity [26].

Cross-linked enzyme aggregates (CLEAs) utilise the same cross-linking principle as CLECs, but without the time-consuming crystallisation process and the need for purified enzymes (Figure 1-3). Enzyme aggregates are made through normal precipitation methods, such as salts or organic solvents and are held together by non-covalent bonding [27]. Enzyme aggregates still have the highly ordered

structure seen in crystallised enzymes, but the process is much simpler. Glutaraldehyde is used to perform the cross-linking reaction for both CLECs and CLEAs in a similar fashion to the cross-linking process undergone by multi-subunit enzymes.

CLEAs can be formed with free enzymes or with enzymes that previously have been immobilised to a support through other means. If the enzymes to be cross-linked were immobilised previously, the aggregation step is unnecessary as the insoluble support takes its place. Additionally, in an industrial setting, CLEAs made from free enzymes are difficult to separate from the substrate, which, in the early stages of the degradation process, most likely will be a suspension [28]. As an example, CLEAs have been made using enzymes immobilised onto silanised ferrous magnetic particles, which were then cross-linked using glutaraldehyde [28].

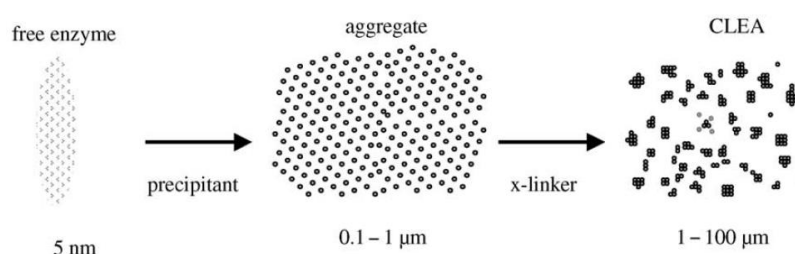


Figure 1-3: The process of creating cross-linked enzyme aggregates and the size changes the particles go through [26].

### *Self-assembled monolayers (SAMs)*

Organic molecules that spontaneously assemble into an ordered structure on a surface through adsorption are known as self-assembled monolayers (SAMs). SAMs can then facilitate the immobilisation by covalent attachment of the enzyme of interest [29]. Biological molecules that self-assemble have a headgroup that shows affinity to the inorganic support and a tail that is capable of forming a covalent bond with reactive enzyme side-chains under the correct reaction conditions [30, 31]. A SAM of densely-packed alkanethiolates on gold has been used to immobilise a cutinase that remained stable and active, with no non-specific adsorption of the enzyme to the SAM [32].

Thiol-containing molecules adsorbed to gold are a common way of producing SAMs. Flat gold or gold nanoparticles can be used as a support and the resulting SAMs are oxide free, clean and flat [31]. The

sulfur atom of the thiol undergoes a chemisorption reaction with the gold surface, forming a strong thiolate-gold bond [31]. However, as with other methods of covalent immobilisation, enzymes immobilised to SAMs can show a reduction in activity due to the random nature of the reaction [33].

## **Solid Binding Peptides as a New Immobilisation Tool**

Solid-binding peptides (SBPs) are short amino acid sequences that bind strongly and selectively to solid, mostly inorganic, support materials such as glass, silica, or gold. Metals, metal oxides, minerals, carbon-based materials, and semiconductors are some of the inorganic materials that have SBPs that bind to them specifically [29]. The SBP is fused genetically to the enzyme at the sequence level (either N-terminal or C-terminal) and expressed as a fusion protein. In most cases, SBPs are able to direct the orientated immobilisation of enzymes while still retaining catalytic activity. No chemical reaction is necessary and the enzymes retain their biological function, combining the most desirable features of both non-specific adsorption and covalent modification.

SBPs bind to solid materials through non-covalent interactions such as electrostatic interactions, polar interactions, hydrophobic interactions, or hydrogen bonds [29]. Their amino acid sequences contain residues that promote binding to specific materials. For example, gold-binding peptides contain a high proportion of thiol-containing cysteine residues, which show semi-covalent binding affinity to gold atoms [34]. Materials that carry a surface charge tend to bind SBP sequences that contain residues of the opposite charge through electrostatic interactions. However, the exact binding mechanisms are poorly understood due to the complexity of the interface between the peptide and the inorganic support [29]. SBPs are able to adopt many different three-dimensional conformations due to sequence features that promote structural disorder [6]. Their sequences are too short to have any defined tertiary structure so multiple conformations are possible [35], but there is usually one conformation that promotes maximum contact between key residues and the inorganic surface [29]. SBPs that bind to the same inorganic material display some sequence similarity but due to the heterogeneity of many support surfaces and varied peptide-support interactions, it is difficult to determine a clear binding sequence consensus [35].

SBPs are selected using combinatorial display technologies such as phage display or cell-surface display. Phage display is the most common method as it allows for the binding affinities and specificities of peptides to be assayed before the time and resources are invested into expressing and purifying them in the quantities needed for conventional affinity determinations [36] (Figure 1-4). However, phage display requires a secondary host to amplify the peptide(s) of interest while cell-surface display does not [35]. Random peptide libraries are displayed on phage coat proteins or cell membranes and screened against the support of interest. Any peptide sequences that display binding affinity remain bound to the support and are collected. In phage display, the phage particles propagate in a host *Escherichia coli*, and in cell surface display, the cells reproduce as normal. The peptides displaying binding affinity undergo subsequent rounds of selection ('biopanning') under increasingly stringent wash conditions until only the peptides displaying the strongest binding affinity are retained. They are collected from the support and sequenced [37]. Selection of SBPs by phage display is performed under laboratory conditions (ambient temperatures, dilute laboratory buffers), which may not translate well to performance in downstream applications under industrial conditions (high temperatures, concentrated buffers). SBPs may become unstable under harsh industrial conditions, resulting in degradation or dissociation from their supports. Peptide libraries destined for commercial conditions should be screened under industrial conditions to select SBPs that are stable initially so as to minimise the possibility of instability.

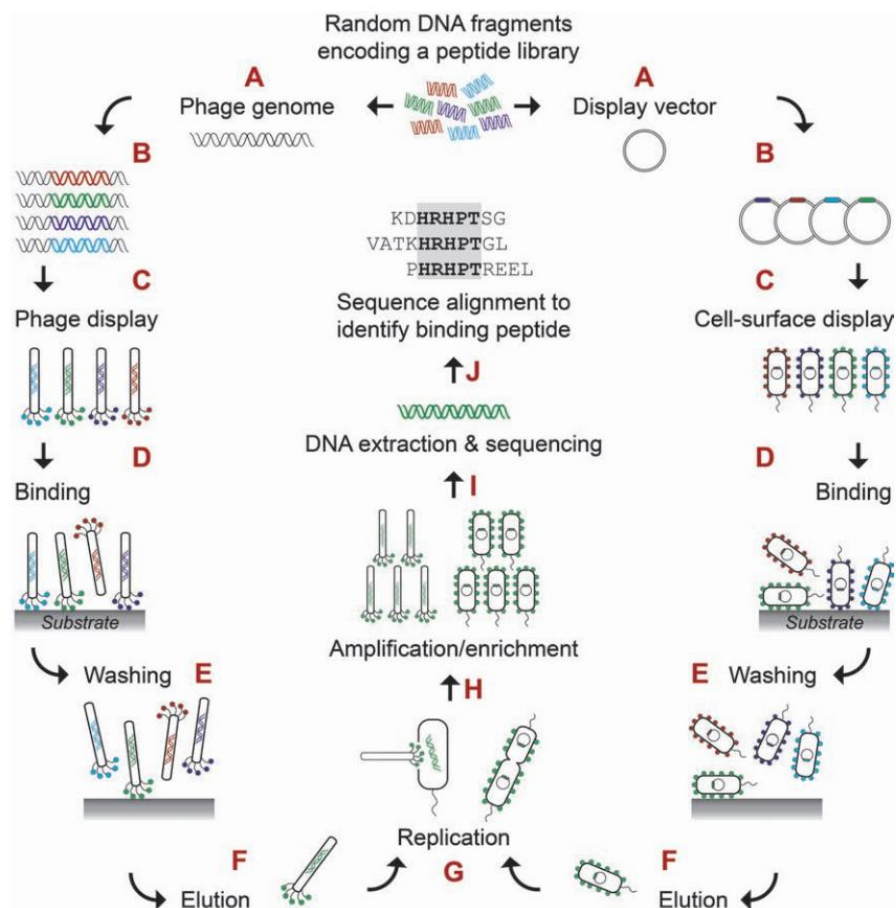


Figure 1-4: An overview of the process of phage display and cell-surface display. Random peptide sequences are displayed on phage coat proteins or cell membranes, and selected against the support of choice [35]. A; carrier DNA for the peptides, either the phage genome or the display vector, B; carrier DNA with peptides inserted, C; the random peptides are displayed on the phage coat or cell surface, D; displayed peptides are mixed with the substrate and allowed to bind, E; the washing step to remove weak and non-specific binders, F; elution of the strongest binders from the substrate, G; replication of the strongest binders, through infection of *E. coli* or normal cell division, H; amplification of the selected peptide(s) through continued replication of the cell or phage, I; extraction and sequencing of DNA containing the enriched peptide sequence, J; computational sequence alignment to identify the putative binding peptide.

Novel SBP sequences also can be designed *in silico* based on known SBP sequences. Random peptide sequences are generated computationally and their sequence similarity to known SBPs with common binding affinities calculated [35]. The higher the sequence similarities the sequences generated show to known SBPs, the higher is the expected binding affinity to the support of interest [35].

### SBP applications in nanobiotechnology

Nanomaterials can be constructed using 'top-down' or 'bottom-up' fabrication. Top-down fabrication uses lithographic techniques to construct nanoscale materials from macroscopic starting materials,

while bottom-up fabrication uses molecular recognition and self-assembling biomolecules to form larger structures [29]. Bottom-up strategies provide higher spatial resolution, fewer surface imperfections and degradation and high turnover compared to top-down approaches, as well as being less cost-intensive than top-down approaches [29]. SBPs can be used in the 'bottom-up' strategy to facilitate the construction of functionalised nanomaterials, as well as providing an organic coating which the biological environment can safely interact with. Several nanomaterials, such as quantum dots and carbon-based nanomaterials have been shown to cause cytotoxicity *in vivo* and *in vitro* [38, 39]. Important factors affecting how a nanoparticle interacts with a biological environment include surface charge, functional groups, size, shape and surface area, hydrophobic/hydrophilic interactions, and tendency to form aggregates [40]. Nanoparticles can be coated with SBPs to increase biocompatibility and reduce toxicity to help overcome these problems [29]. The SBPs bind to the nanomaterials in a highly specific manner and generally are functional under biological conditions, avoiding the production of immunogenic or cytotoxic responses. SBPs also have been used in the immobilisation of a variety of biomolecules such as antibodies, enzymes and antigens in a range of sensitive diagnostic and therapeutic applications, such as biosensors, chemosensors, and targeted drug delivery [29].

SBPs have been used in the fabrication of nanoscale objects (Figure 1-5). The physical and chemical properties of nanomaterials can change depending on their size and morphology, which affects the ability of the nanomaterial to adsorb and desorb in a reaction [41]. Morphologically-distinct nanocrystal faces have shown different activity levels due to different adsorption rates of ions [41]. It is thought that the growth of nanocrystals is driven by the kinetic energy necessary to fabricate the different faces. This directs the formation of shapes comprised of low-energy faces in preference to high-energy ones [42]. 'Capping agents' such as SBPs have been shown to direct the formation of nanocrystals. SBPs bind to a particular face and lower its surface energy, which can direct nanoparticle material towards a face that may otherwise not have been able to participate in fabrication [43]. SBP capping has been used to fabricate palladium nanocrystals [44], platinum nanocrystals [42], cobalt nanorods [42], cadmium selenide nanocrystals [45] and zinc sulfide nanoparticles [45].



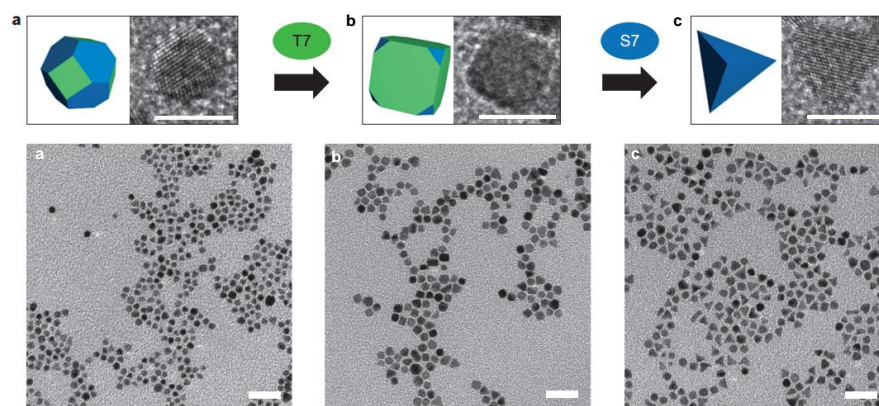


Figure 1-5 : Different 3-dimensional nanostructures fabricated through the use of peptide capping agents [42]. T7 and S7 are different capping peptides, and switching between them leads to different structures. a; unmodified platinum nanocrystal octahedrons, b; T7-induced nanocrystal cubes, c; S7-induced nanocrystal tetrahedrons. Scale bars: 5nm (top images), 20nm (bottom images).

### Silica-binding SBPs

Several SBPs have been reported that display specific binding affinity to silica-based inorganic matrices. Sequences of silica-binding SBPs contains a high proportion of basic amino acid residues (especially arginine), which confer low hydrophobicity and high net charge [6]. Additionally, peptides showing affinity tend to have a low amount of aromatic and hydrophobic residues, both of which confer structural rigidity [37].

A silica-binding SBP with the sequence MSPHPHPRHHHT was used to immobilise a *Xanthobacter autotrophicus* haloalkane dehalogenase expressed in *E. coli* onto magnetic nanoparticles (MNP, Figure 1-6). Superparamagnetic nanoparticles consisting of an iron core and a ferric oxide shell were functionalised by a silica coating. Recombinant His-tagged SBP-haloalkane dehalogenase fusion protein was affinity purified from *E. coli* cell lysate and immobilised onto silanised MNPs [46]. Binding of His-tagged SBP-haloalkane dehalogenases occurred at a higher rate than when only the His-tag was used [46]. It was shown also that His-tagged SBP-haloalkane dehalogenase could adsorb to the MNPs directly from the cell lysate, outcompeting host proteins showing binding affinity through non-specific adsorption [46].

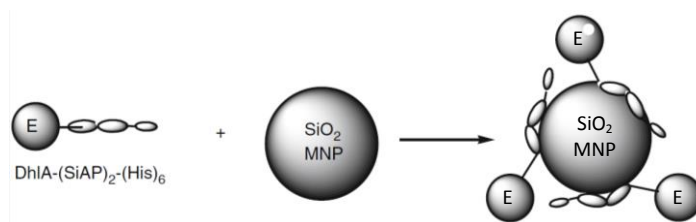


Figure 1-6: A silica-binding SBP (SiAP) used for the immobilisation of haloalkane dehalogenase (DhlA) onto silicon dioxide magnetic nanoparticles. His-tagging was used to purify the enzyme from the cell lysate. The enzyme is represented by 'E' [46].

Another silica-binding SBP isolated from *Bacillus cereus* spore coat protein CotB1 has been used as a fusion tag for affinity purification of recombinant proteins. This SBP was selected as a result of the observation that *B. cereus* spores collected silica deposits as a layer of nanoparticles. The sequence was identified through gene disruption analysis rather than through combinatorial display technologies [47]. The SBP itself is a sequence 14 amino acids long (SGRARAQRQSSRGR) from the C-terminal end of CotB1 [47]. This 14 amino acid sequence contained a high number of positively charged residues (particularly arginine and serine), which is characteristic of silica-binding peptides [47]. It was used as a 'Si-tag' to purify GFP-CotB1 fusion proteins from *E. coli* cell lysate using  $\alpha$ -quartz silica particles. Purification using the Si-tag showed comparable efficiency to conventional affinity purification techniques, but at a reduced cost [47]. The Si-tag can also be used under reducing conditions, which allows for the purification of proteins expressed in inclusion body aggregates [47].

*E. coli*, *Pseudomonas aeruginosa*, and *Pseudomonas putida* ribosomal L2 proteins were shown to bind silica 20- to 100-fold more strongly than poly-Arg tags (as measured by  $K_d$  values) [48]. L2 was identified as a silica-binding protein by screening the cell lysate against silicon particles, and two SBPs were identified through L2 deletion mutants fused to GFP [48]. The SBPs were located at the N- and C-termini of L2 and were comprised of two amino acid sequences, 60 (MAVVKCKPTSPGRRHVVKVNPVLHKGKPFAPLLEKNSKSGGRNNNGRITTRHIGGHKQ) and 70 (VLGKAGAARWRGVRPTVRGTAMNPVDHPHGGGEGRNFGKHPVTPWGVQTKGKKTRSNKRTDKFIVRRRSK) amino acids in length, respectively [48]. The SBPs contained a high proportion of positively-charged residues making them strong binders.

Car9 is a silica-binding SBP consisting of 12 amino acids (DSARGFKKPGKR) sourced from *E. coli* thioredoxin. It was known previously as a graphite-binding peptide that bound through electrostatic interactions (between basic lysine/arginine and negatively charged hydroxyl and carbonyl groups on the support) [49]. It was hypothesised that Car9 would also show binding affinity to silica-based materials since the SiO<sub>2</sub> component contains hydroxyl-terminated silanol groups [49]. Car9 proved to be useful as a Si-tag for the rapid purification of tagged GFPmut2. Using a silica-gel column, it was possible to go from clarified cell extract to purified protein in less than 15 minutes [49].

### **Matrices and supports for silica-binding SBPs**

There are a number of qualities an inorganic material should have to be considered as a support for enzyme immobilisation. The material should have a large internal surface to provide a good geometric compatibility with the protein [4]. The support also should have a high density of reactive groups such as charged groups for electrostatic interactions, non-polar groups for hydrophobic interactions, or functional groups for conjugation with reactive side chains on the protein [4]. The reactive groups must not contribute any significant steric hindrance to the reaction and the support and the protein must be chemically compatible [4]. If the support is activated as part of the immobilisation, it must be rendered inert with ease after the reaction is complete [4]. If not, the support must be inert from the start. Some supports that have these characteristics include zeolites, agarose beads, porous glass, and epoxy resins [4].

#### *Patterned substrates*

Micro-patterned substrates can be used to direct the immobilisation of enzymes in highly specific arrays for the fabrication of nanoscale sensors, protein chips and microarrays. Previous work has demonstrated the creation of a gold support functionalised with alkanethiols attached by micro-contact printing to create a self-assembled monolayer for the patterned immobilisation of alkaline phosphatase [50] (Figure 1-7).

However, SAMs and other conventional immobilisation techniques do not discriminate between different supports in close proximity, so their use in creating patterned substrates is constrained to a limited range of supports [29]. Nanofabrication techniques rely on the highly selective

functionalisation of multiple materials patterned at the nanoscale but many headgroups used to fabricate SAMs exhibit low material selectivity.

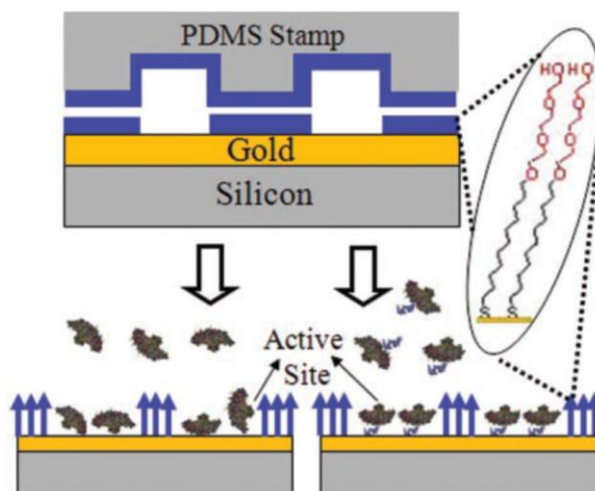


Figure 1-7: Micro-contact printing of a gold substrate with alkanethiols to create a patterned substrate. Alkanethiol molecules exclude the gold-binding peptides located in the enzyme sequence and the enzymes are forced to immobilise in patterns [50]. PDMS; polydimethyl siloxane.

In contrast, SBPs are highly material-selective and can be used to fabricate nanomaterials that discriminate between different substrate materials [29]. SBPs have been used to functionalise gold micro-patterned silica. Silica wafers were patterned with gold using photolithographic techniques, facilitating immobilisation of fluorescent nanoparticles using two different SBPs showing binding affinity to silica and gold. Different fluorescent nanoparticles for each SBP showed that immobilisation occurred successfully in a material-specific manner on a micro-patterned substrate [51].

### *Nanomaterials*

Nanofibres, nanoparticles, nanosheets, nanotubes, nanocomposites and nanopores are some of the nanomaterials that have been used in enzyme immobilisation [52]. Nanomaterials used for immobilisation are usually functionalised beforehand with appropriate functional groups or other biorecognition molecules [53]. Physical adsorption of the enzyme also can be done onto unmodified nanomaterials [54]. Porous nanomaterials allow for immobilisation of enzymes inside the nanopores, restricting access of the enzyme to any external interface that may cause denaturation, such as gas bubbles introduced while stirring [4]. Porous nanoparticles provide this extra layer of 'operational

stability' in addition to the improved stability already offered by immobilisation [4]. Magnetic nanoparticles can be removed easily from a reaction medium using a magnetic field, but they lose the advantages of porous nanomaterials [4]. A compromise between these two types of nanomaterials involves functionalising magnetic nanoparticles with a coating of porous nanomaterials, which allows for a wider range of SBPs (i.e. displaying affinity to non-magnetic materials) to be used for immobilisation.

### **Bulk-based silica matrices**

Although the support materials discussed previously have shown success in laboratory environments and have applications in nanobiotechnology, they are not suitable as bulk, low-cost matrices for enzyme immobilisation on an industrial scale. Lithographic printing processes to pattern nanomaterials can become expensive, and can be quite time-consuming, as can be nanoparticle functionalisation. Most of the cost of purification and immobilisation techniques comes from the stationary phase (i.e. the matrix and support) [49]. Using naturally-occurring earth-abundant materials as support matrices is a desirable solution to bringing down production costs [49]. Zeolites and other similar silica-based materials are potential bulk, low-cost matrices for immobilisation of industrially relevant enzymes. They do not require any chemical functionalisation to become useable, and can be synthesised or mined cheaply. In particular, silica can be tailored easily into a large range of porous surfaces, surface functionalities, and processing conditions [55]. Mesoporous nanomaterials are used because of their high surface area, controlled porosity and simple adsorption and desorption [56]. Silica-based supports show high mechanical strength and microbial resistance compared to other polysaccharide-based adsorbents [57]. This makes silica-based materials well-suited for industrial-scale processes.

Zeolites are highly ordered aluminosilicate compounds that can be synthesised as nanoparticles of various sizes. They are a common industrial adsorbent that are mechanically and chemically resistant over a wide range of temperatures and pH values [6]. Zeolites carry a net negative charge, which gives peptide sequences containing positively charged residues a high binding affinity towards them [6]. The aluminium and silicon atoms form a three-dimensional, porous network containing two distinct 'faces' [58] (Figure 1-8). Natural zeolites are known to have a porosity of up to 0.3mL/g [58]. Zeolites also can be synthesised with different ratios of aluminium and silica. Reduction of the amount of aluminium in the zeolite reduces the affinity of the zeolite for water, as the silica exists as

neutral  $\text{SiO}_2$  [59]. Removing aluminium ions removes the only charged species, reducing the polarity of the entire structure.

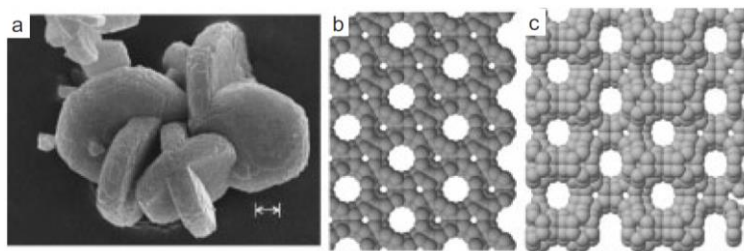


Figure 1-8: Electron microscopy images of the two different face of EMT (Ecole Supérieure Mulhouse Two) zeolite. Image a) shows entire disc-shaped particles, image b) shows the face consisting of flat hexagonal crystals, and image c) shows the thin side face [58]. Scale bar =  $1\mu\text{m}$ .

Particle size is an important consideration when selecting a zeolite as an inorganic support. The curved surface of the zeolite nanoparticles prevents lateral protein-protein interactions that can induce denaturation, while the surfaces of larger nanoparticles can approach a ‘pseudo-flatness’ [46]. Conversely, nanoparticles that are too small will not produce sufficient electrostatic forces to bind to SBPs. Previous research indicates particles of approximately  $1\mu\text{m}$  in diameter are ideal [37].

## The project

### Cell-free biocatalytic modules

Immobilised enzymes have the potential to be assembled into biocatalytic pathways to produce an economically-desirable product in a cell-free environment. Cell-free pathways (*in vitro*) (Figure 1-9) can be compared to traditional biotechnology methods using living cells (*in vivo*). Using living cells to produce a desirable biocatalyst means that a portion of the carbon source will be sequestered by the cell for its own growth and metabolic needs [56]. Energy provided by the carbon source will be diverted for self-duplication, maintenance, or other metabolic pathways that have common intermediates [56]. These factors may contribute to low product yields. Metabolic engineering to optimise living cells is an option for improving the yields of *in vivo* systems. Desirable genes can have their expression levels enhanced, while undesired genes can be deleted [60]. However, this engineering can lead to genetic imbalance, as artificially engineered cells may lack the naturally evolved regulatory mechanisms found in natural metabolism [60]. In contrast, *in vitro* systems do not

suffer from many of these restrictions. Designing a pathway using a cell-free, bottom-up approach provides engineering flexibility unhindered by biological membranes, restrictions from cell viability and physiology and the inherent metabolic complexity of living cells. High product yields are possible without energy being diverted into cell duplication or side products [56]. Reaction conditions can be broader in terms of temperature and organic solvents used since it is not necessary to use conditions that favour cell survival. *In vitro* systems are ideal for producing compounds that normally would be toxic to cells and for products that are not secreted and require cell lysis for collection in an *in vivo* system [61]. High enzyme loadings are possible in *in vitro* systems as space is not taken up by cellular components and *in vitro* systems provide a less crowded reaction environment overall [62]. With the removal of biological membranes, *in vitro* systems allow immobilised enzymes direct access to the substrate and the reaction medium, and the entire reactor volume is available [61]. *In vitro* systems are easier to scale up for industrial production than *in vivo* systems. However, living systems are better able to balance and supply any coenzymes necessary (e.g. ATP, NADH) [56].

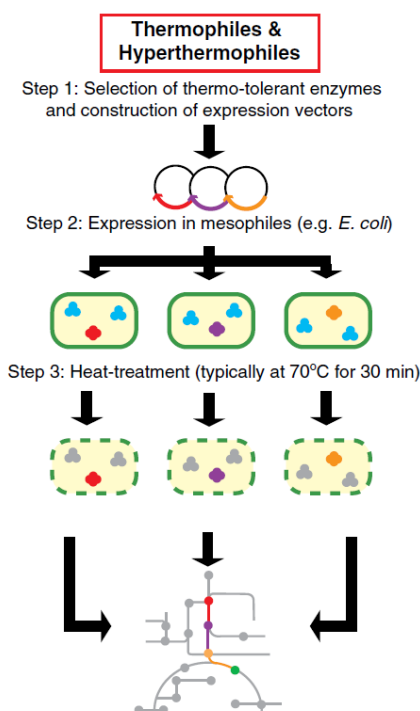


Figure 1-9: Construction of an *in vitro* pathway using biocatalytic modules. The bottom of the flow chart shows the position of the assembled pathway within the organism's natural metabolism where undesirable side reactions that may occur are eliminated [60].

Cell-free systems can be used to assemble both natural and non-natural pathways. High-demand products such as protein drugs, biocommodities, fine chemicals, and biomaterials can be synthesised using cell-free biocatalytic modules assembled into the necessary pathways [63]. Cell-free systems

can be assembled in two different ways. Enzymes can be sourced from a whole-cell extract, or purified enzymes from different sources can be mixed together [63]. Whole-cell extracts are easier to prepare than purified enzymes from different sources, but they have a short half-life [63]. Purified enzyme systems are more labour-intensive than whole-cell extracts, but the separate biocatalytic modules can be stabilised after each immobilisation process with protocol that is optimised for each enzyme [63]. So far, labelled purine nucleotides, carbohydrates, circular DNA, modified RNA, liposomes and proteins have been synthesised using cell-free biocatalytic modules assembled into natural and non-natural pathways [56].

### **SBP-mediated biocatalytic module design**

SBPs have been used mainly as molecular tools for functionalisation of nanomaterials and little is known about their potential use for the immobilisation of enzymes and their applications in industrial-scale biocatalysis. Silica, zeolite and other mesoporous silica-based materials are considered the most suitable inorganic matrices for the immobilisation of enzymes [55, 57]. They are inexpensive and robust, with high mechanical strength, chemical and microbial resistance, and high surface area [6]. They are stable under wet or dry conditions, and the Si/Al ratio of zeolites can be modified during synthesis to create zeolites that are either basic or acidic [6]. However, unmodified silica as an inorganic support is unusual, as supports are usually functionalised prior to immobilisation of a biomolecule, both in single and multiple enzyme immobilisation [6]. So far there is only one report on the use of SBPs for the immobilisation of thermostable enzymes [37].

The SBP used in this project is a silica-binding SBP, referred to as a 'Linker' because it acts as a molecular linker between the enzyme and the support. The Linker sequence was selected against specific synthetic zeolites using cell surface display [58]. The peptide sequence consists of four repeats of VKTQATSREEPPRLPSKHRPG, followed by the first seven residues repeated a fifth time. The theoretically-determined pI of the Linker is 10.90, and the overall charge, calculated from the number of positively and negatively charged residues, is +3 [29]. It was assumed previously that the binding mechanism of this SBP to zeolite was due to the peptide being able to recognise different spatial configurations of the different faces of three-dimensional zeolite nanoparticles [58]. Dye-exclusion experiments indicated that an SBP-alkaline phosphatase fusion protein excluded dye bound to one zeolite face, but not the other [58]. If this was the case, it can be expected that the SBP would display highly selective zeolite-matrix binding. However, further work using an immobilised



*Streptococcus* Protein G found that the SBP showed binding affinity to a large range of zeolites, both natural and synthetic [6]. Binding to such a large range of silica-based matrices indicated that binding affinity may be due to the SiO<sub>2</sub> component [6].

This is a pilot project and proof of concept to determine the potential suitability of this type of cell-free biocatalytic module(s) for industrial applications. Biocatalytic modules are designed using a silica-binding SBP and low cost bulk silica-based matrices. Single biocatalytic modules consist of one type of enzyme immobilised per matrix molecule, while mixed biocatalytic modules consist of more than one (Figure 1-10: Diagrammatic representation of biocatalytic modules consisting of enzymes and a solid matrix. Four modules are represented, three single modules and one mixed module.). Biocatalytic modules can be used to replace industrial chemical catalysts due to their high specificity and high efficiency under mild reaction conditions [56].

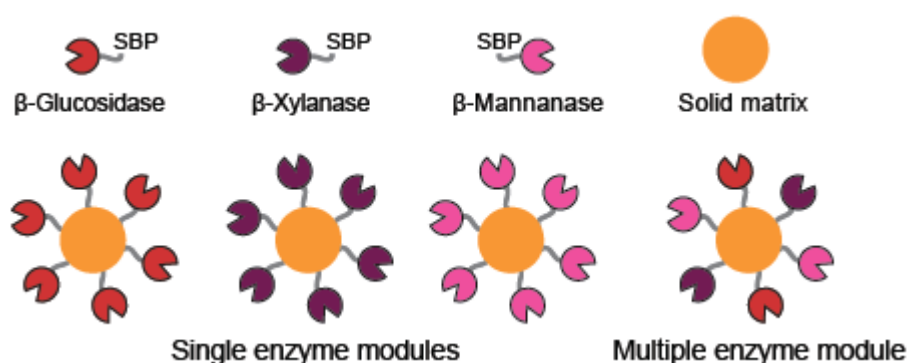


Figure 1-10: Diagrammatic representation of biocatalytic modules consisting of enzymes and a solid matrix. Four modules are represented, three single modules and one mixed module.

We selected three thermostable enzymes, which are optimally active above 60°C. Thermostable enzymes have a number of advantages over mesophilic enzymes. They can be purified easily from the mesophilic expression host by heat denaturation and undesired side reactions are eliminated. The resulting biocatalytic modules are expected to be highly selective and stable.

The main focus of this study is  $\beta$ -glucosidase, the last enzyme in the classical cellulose degradation pathway. Unlike the other cellulases in the pathway,  $\beta$ -glucosidase cannot be recycled by adsorption

to fresh substrate, so it is a priority for immobilisation [64].  $\beta$ -glucosidase has been shown to adsorb poorly to lignocellulosic substrates, minimally or to a far lesser degree than other cellulases [64]. This study focuses particularly on the effect that incorporating the silica-binding Linker peptide has on the activity and function of the  $\beta$ -glucosidase, providing groundwork for future studies on the immobilisation of a cellulose degradation pathway.

To further complement this work, a thermostable  $\beta$ -mannanase (ManA) and  $\beta$ -xylanase (XynB) from *Dictyoglomus thermophilum* were used to supply additional data on the functionality of the Linker. Both enzymes are hemicellulases that catalyse the hydrolysis of the polysaccharides xylan (1,4-linked  $\beta$ -D-xylopyranosyl residues) and mannan (1,4-linked  $\beta$ -D-mannopyranosyl residues), respectively. Hemicellulases, in combination with cellulose-degrading enzymes, play an important role in the efficient degradation of plant biomass.







In this study we demonstrate the application of a silica-binding SBP-mediated immobilisation of industrially-relevant enzymes onto a bulk and low-cost solid zeolite matrix. Additional introduction of cross-linking to the immobilised enzymes into individual and mixed CLEAs further highlight the potential of this platform technology to translate well into industrial-scale processes.

## Chapter 2 Materials and Methods

### Transformation of *Escherichia coli* competent cells

The expression plasmids pET22-L-*bglA* and pET22-L-*xynB* contained the Linker sequence (L) genetically fused to the N-terminus of *Caldicellulosiruptor saccharolyticus*  $\beta$ -glucosidase A (*bglA*) and *Dictyoglomus thermophilum*  $\beta$ -xylanase B (*xynB*), respectively. The pET22-ManA-L expression plasmid contained the Linker sequence fused to the C-terminus of *C. saccharolyticus*  $\beta$ -mannanase A (*manA*). The location of the Linker on each enzyme was chosen due to the location of the catalytic domain of each enzyme. The catalytic domains of XynB and BglA are N-terminal [65, 66], while the catalytic domain of ManA is C-terminal [67]. Recombinant constructs are represented diagrammatically in Table 2-1. These plasmids, in addition to expression plasmids of pET22-*bglA*, pET22-*manA* and pJLA602-*xynB* expressing the enzymes without the Linker sequence were kindly supplied by Dr Andrew Care and Dr Anwar Sunna. Plasmids pET22-L-*xynB*, pJLA602-*xynB*, pET22-*manA*-L, pET22*manA* and pET22-*bglA* were provided in *Escherichia coli* Tuner (DE3) cells as glycerol stocks. The plasmid pET22-L-*bglA* was transformed into competent *E. coli* BL21 cells (Bioline) using 50ng of DNA via heat shock at 42°C for 30 seconds. Plates with Luria-Bertani (LB) agar supplemented with (50 $\mu$ g/mL) carbenicillin were spread with 60 $\mu$ L of culture and incubated overnight at 37°C. Single transformant colonies were obtained from the streak plate and then transferred onto a LB agar plate supplemented with carbenicillin (50 $\mu$ g/mL), 100 $\mu$ L 5-bromo-4-chloro-3-indolyl- $\beta$ -D-galactopyranoside (X-gal, 1M) and isopropyl  $\beta$ -D-thiogalactoside (IPTG, 0.4 mM) to check for colonies expressing the recombinant L-BglA enzyme [68].

Table 2-1: Enzyme constructs with and without Linkers. N<sup>a</sup>; N-terminal Linker, C<sup>b</sup>; C-terminal Linker, N/A; enzyme does not have Linker.

Construction	Function	Source	SBP position
 L-BglA	$\beta$ -glucosidase	<i>Caldicellulosiruptor saccharolyticus</i>	N <sup>a</sup>
 L-XynB	$\beta$ -Xylanase	<i>Dictyoglomus thermophilum</i>	N <sup>a</sup>
ManA-L 	$\beta$ -mannanase	<i>Dictyoglomus thermophilum</i>	C <sup>b</sup>
 BglA	$\beta$ -glucosidase	<i>Caldicellulosiruptor saccharolyticus</i>	N/A
 XynB	$\beta$ -Xylanase	<i>Dictyoglomus thermophilum</i>	N/A
 ManA	$\beta$ -mannanase	<i>Dictyoglomus thermophilum</i>	N/A

### **Recombinant protein expression**

Recombinant enzymes were produced from glycerol stocks of recombinant cells in LB liquid cultures supplemented with carbenicillin (50µg/mL). Recombinant protein expression for all plasmids except XynB were induced by addition of IPTG to a final concentration of 0.4mM. The expression plasmid pJLA602-XynB is a heat-inducible plasmid [69] that requires a shift in growth temperature to 42°C to initiate recombinant protein expression. All cultures were grown with shaking (250 rpm) at 37°C until an OD<sub>600</sub> of between 0.7 and 0.9 was reached followed by induction and the cultures incubated for 4 h with shaking at 37°C (42°C for XynB), then the cells were harvested by centrifugation for 15 min at 4000 x *g* at 4°C and stored at -30°C.

The cells were suspended in ice-cold cell resuspension buffer (TST buffer, 25mM Tris-HCl, 100mM NaCl, 1.25mM EDTA, 0.05% Tween 20, pH 8.0) and the serine protease inhibitor Pefabloc® (5mg, Sigma) and lysozyme (1mg, Sigma) were added. The cells were disrupted by three passages through a French pressure cell at 1000kPa. Benzonase (3µL, Novagen) and Pefabloc® (5mg) were added immediately following French pressing. The cell suspension was centrifuged at 4000 x *g*, for 30 min at 4°C following incubation on ice for 20 min. Then the supernatant obtained was incubated for 30 min at 70°C to denature host proteins and to partially purify the recombinant protein. Heat-denatured proteins were removed by centrifugation at 4000 x *g* for 30 min at 4°C. The supernatant obtained was filtered through 0.45µm and 0.20µm sterile filters (Millipore). The protein concentrations of all enzymes were determined with a NanoDrop 2000 (Thermo Scientific) and adjusted to a final concentration of 1-2 mg/mL. The enzymes were dispensed into 300µL portions and stored at 4°C and at -80°C.

### **Standard zeolite binding assay**

The silica-containing matrix used was synthetic zeolite CBV100 (Zeolyst International, USA). Zeolite (5mg) was washed three times with 500µL washing buffer (1% Triton X-100 in 50mM phosphate buffer, pH 6.0) by vortexing and centrifugation at 10,000 x *g* for 30 s. Soluble, partially-purified enzyme (20µg in 100µL of phosphate buffer) was mixed with the washed zeolite and incubated with rotation for 30 min at room temperature. After centrifugation at 10,000 x *g* for 30 s, the supernatant containing the unbound fraction was removed. The zeolite pellet then was washed three times with

100µl of 50mM phosphate buffer (pH 6.0) by vortexing and centrifugation at 10,000 x *g* for 30 s. Zeolite-bound proteins were eluted from the matrix using 100µL SDS-PAGE loading buffer and incubation at 99°C for 10 min. Fractions containing protein were separated on 4-12 % gradient Bis-Tris Gels (Life Technologies) by SDS-PAGE and identified with Coomassie Brilliant Blue staining.

### **Standard enzyme assays**

All reaction mixtures consisted of an appropriate amount of enzyme (20µL) and their respective substrate (80µL). Reactions were prepared in triplicate and incubated at 80°C for 10 min. Each enzyme was diluted to a concentration that was not substrate limited during the assay reaction. For comparison and convenience, all enzyme activities are expressed as % maximal activity.

β-glucosidase activity was assayed using 0.5mg/mL *p*-nitrophenyl-β-D-glucopyranoside (pNPGluc, MP Biomedicals) substrate in the appropriate buffer (buffer and pH dependent on the assay type). The assay reactions were terminated by addition of 100µL 1M Na<sub>2</sub>CO<sub>3</sub> at room temperature and the absorbance of the released *p*-nitrophenol was measured at 405nm using a PHERAstar FS 96-well plate reader (BMG Labtech).

β-xylanase and β-mannanase activities were assayed using 0.5% (w/v) oat spelt xylan (OSX, Sigma) and locust bean gum (LBG, Sigma) substrates in the appropriate buffer (buffer and pH dependent on the assay type). The reducing sugars released were measured using the dinitrosalicylic acid (DNS) assay procedure [70] and the absorbance increase generated by the release of 3-amino-5-nitrosalicylic acid was measured at 540nm using the PHERAstar FS 96-well plate reader.

### **Activity characterisation of free enzymes**

The effects of pH and temperature on the free enzyme activities were examined using the partially purified recombinant proteins. The effect of temperature on the reaction rate was determined by incubating the free enzyme with the appropriate substrate in 50mM phosphate buffer, pH 6.0, at temperatures ranging from 40°C to 90°C under standard assay conditions. To determine the optimal pH, the appropriate substrate was prepared in Britton-Robinson buffer [71] (40mM for pNPGluc, 120mM for OSX and LBG) and assayed at different pH values (all pH values were adjusted at the

temperature of the assay) at the optimal temperature for activity. Britton-Robinson buffer was selected for optimal pH measurements as it is a 'universal' buffer capable of adjustment to a wide range of pH values, while phosphate buffer was chosen for optimal temperature measurements due to its resistance to pH fluctuations caused by temperature change. For comparison purposes, phosphate buffer was used in all other assays.

## **Enzyme immobilisation**

### *Zeolite-bound enzymes (zeo-enzyme)*

Zeolite-bound fractions were prepared for each enzyme fused to the Linker (L-BglA, L-XynB and ManA-L) using standard zeolite binding assays. They were performed with each of the three partially purified Linker-enzymes without the final SDS heat elution step, after which the final insoluble zeolite-bound fraction was resuspended in 50mM phosphate buffer, pH 6.0, for storage at 4°C.

### *CLEAs of free enzymes (enzyme<sub>CLEAs</sub>)*

CLEAs of each free enzyme (BglA, XynB and ManA with and without Linkers) were prepared by a combined one-step ethanol precipitation and cross-linking strategy. Glutaraldehyde (0.5, 3 and 10% v/v) in chilled 100% ethanol to a total volume of 9mL was added to 1mL of each of the partially purified free enzymes and incubated overnight at 4°C without shaking. The enzyme<sub>CLEAs</sub> formed were centrifuged for 4000 x *g* for 30 min at 4°C, and the supernatant tested for residual enzyme activity. The absence of detectable activity in the supernatant was taken as an indication that aggregation and cross-linking had gone to completion. The enzyme<sub>CLEAs</sub> were washed three times in 50mM phosphate buffer (pH 6.0) to remove any unreacted glutaraldehyde and stored in the same buffer at 4°C.

### *CLEAs of zeolite-bound enzymes (zeo-L-enzyme<sub>CLEAs</sub>)*

CLEAs of each enzyme fused to the Linker (L-BglA, L-XynB and ManA-L) were prepared using standard zeolite binding assays. They were performed with each of the three partially purified Linker-enzymes without the final SDS heat elution step and cross-linked using 100µL glutaraldehyde (0.5, 3 and 10% v/v). After incubation at 4°C with rotation for 1.5 h, the resulting zeo-L-enzyme<sub>CLEAs</sub> were washed

three times with 500 $\mu$ L of 50mM phosphate buffer (pH 6.0) to remove any unreacted glutaraldehyde and stored in the same buffer at 4°C.

A mixed zeo-L-enzyme<sub>CLEAs</sub> was prepared using an initial mixture containing 100 $\mu$ L of each Linker-enzyme (L-BglA, L-XynB and ManA-L) in a single zeolite standard binding assay as described above. The resulting mixed zeo-L-enzyme<sub>CLEAs</sub> were resuspended in 100 $\mu$ L 50mM phosphate buffer (pH 6.0). A 10 $\mu$ L sample was wet-mounted onto a glass slide for light microscopy to ascertain that the cross-linking reaction had been successful.

### **Recycling immobilised enzymes**

Recycling assays were performed with three forms of the immobilised enzymes (zeo-enzymes, enzyme<sub>CLEAs</sub> and zeo-L-enzyme<sub>CLEAs</sub>). Each enzyme was incubated with its appropriate substrate under standard assay conditions. After an incubation period of 10 min, each reaction tube was centrifuged briefly to pellet the immobilised enzyme and the supernatant was transferred to a fresh tube for the addition of the stopping reagents DNS or Na<sub>2</sub>CO<sub>3</sub>. Fresh substrate was added to each immobilised enzyme and the standard assay was performed again. The immobilised enzymes were recycled (reused) in this manner until their relative enzyme activity decreased to 50% of their initial activity.

### **Multiple substrate hydrolysis**

To determine whether the mixed zeo-L-enzyme<sub>CLEAs</sub> were capable of carrying out their hydrolysis reactions, each of the constituent enzymes (L-BglA, L-XynB and ManA-L) in the mixed and individual zeo-L-enzyme<sub>CLEAs</sub> were tested for activity against each substrate (oat spelt xylan, locust bean gum, and pNPGluc) under the standard assay conditions. The relative activity of the mixed zeo-L-enzyme<sub>CLEAs</sub> against each substrate was calculated as a percentage of the activity of the individual zeo-L-enzyme<sub>CLEAs</sub> against the same substrate.

### **Scanning electron microscopy**

Samples of zeo-L-BglA<sub>CLEAs</sub> (5 $\mu$ L) were snap frozen and lyophilised overnight onto electron microscopy coverslips and mounted onto adhesive coverslip stands. The samples were gently agitated with air to

remove loose particles, after which they were coated in gold using an Emitech K550 Gold Sputter Coater Unit. A JEOL-SM-6480 scanning electron microscope was used to image the samples.



## Chapter 3 Results

### Recombinant protein expression

Enzymes with and without the Linker were expressed using *E. coli* BL21 and *E. coli* Tuner (DE3) as expression hosts. The expression level of all enzymes was sufficient to obtain enough soluble recombinant proteins for further studies (5-10mL at 1-2 mg/mL) and no further optimisation was undertaken. The soluble protein fractions were used for partial purification through a heat denaturation step to remove host proteins. SDS-PAGEs containing total, soluble and insoluble proteins fractions for each expressed enzyme are shown in Figure 3-1.

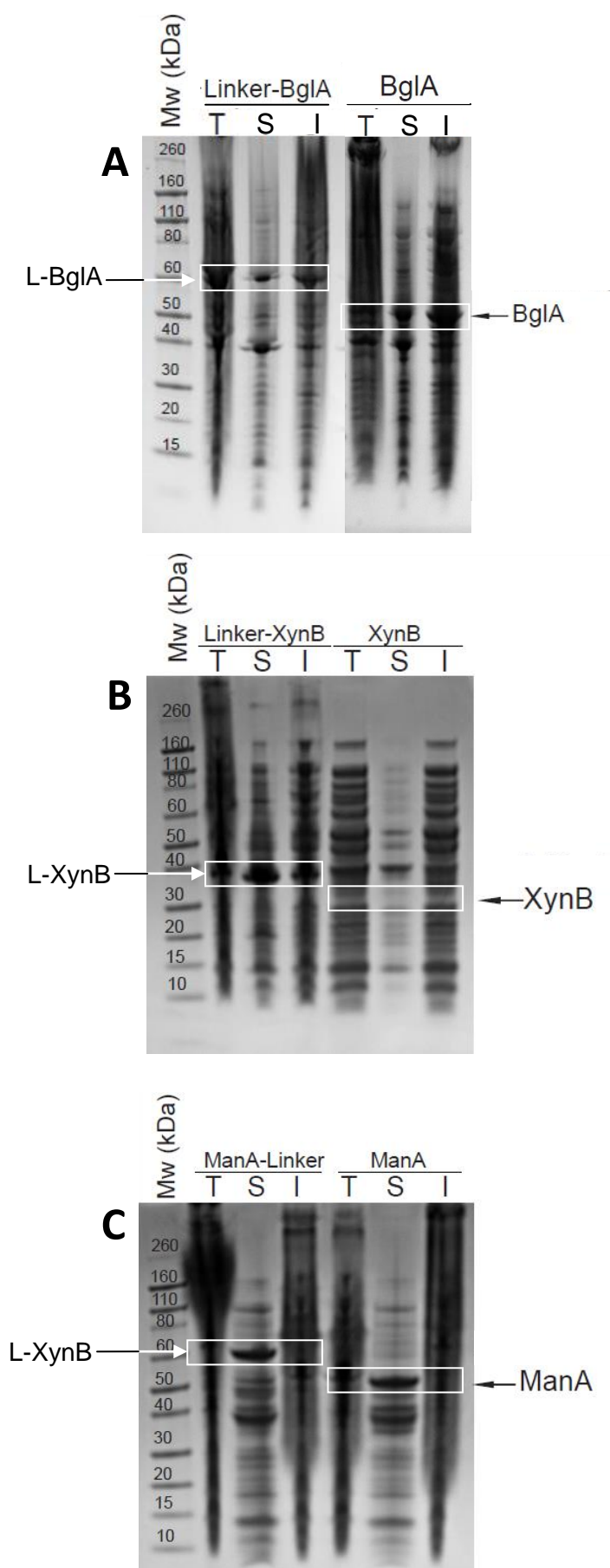


Figure 3-1: SDS gels of total, soluble and insoluble protein for enzymes with and without the Linker prior to partial purification by heat denaturation. (A) BglA and L-BglA, (B) XynB and L-XynB, (C) ManA and ManA-L, 28  
T; total protein fraction, S; soluble protein fraction, I; insoluble protein fraction.

### Activity characterisation of free enzymes

Optimal pH and temperatures were determined for each of the free enzymes using standard activity assays. All partially-purified free enzymes with and without the Linker were active between 40°C and 90°C, with optimal activity at 80°C, indicating that the presence of the Linker did not affect the temperature optimum of the enzymes (Figure 3-2). No changes in the overall activity profile over the temperatures tested were observed with BglA, L-BglA (Fig. 3-2A), ManA and ManA-L (Fig. 3-2C). However, L-XynB displayed 60% more activity at 90°C than its counterpart without the Linker, XynB (Fig. 3-2B)

The presence of the Linker affected the optimal pH of the free enzymes (Figure 3-3). BglA with and without the Linker are active between pH 3.0 and 9.0 and display the same optimum at pH 6.0, but L-BglA has a broader pH curve than BglA. L-BglA activity remains high at pH 7.0, as it is 40% more active than its counterpart without the Linker, BglA (Figure 3-3A). XynB with and without the Linker are active between pH 5.0 and 9.0, with optimal activity at pH 7.0. L-XynB also displays a broader activity range compared to XynB, with 20% more activity at pH 8.0 (Figure 3-3B). ManA with and without the Linker are active between pH 4.0 and 7.0, with ManA optimally active at pH 6.5, and ManA-L optimally active at pH 6.0 (Figure 3-3C). Of all the enzymes tested, ManA-L is the only one that displayed a change in its optimum pH instead of just broadening the activity range. This change was attributed to the presence of the Linker in the fusion protein.

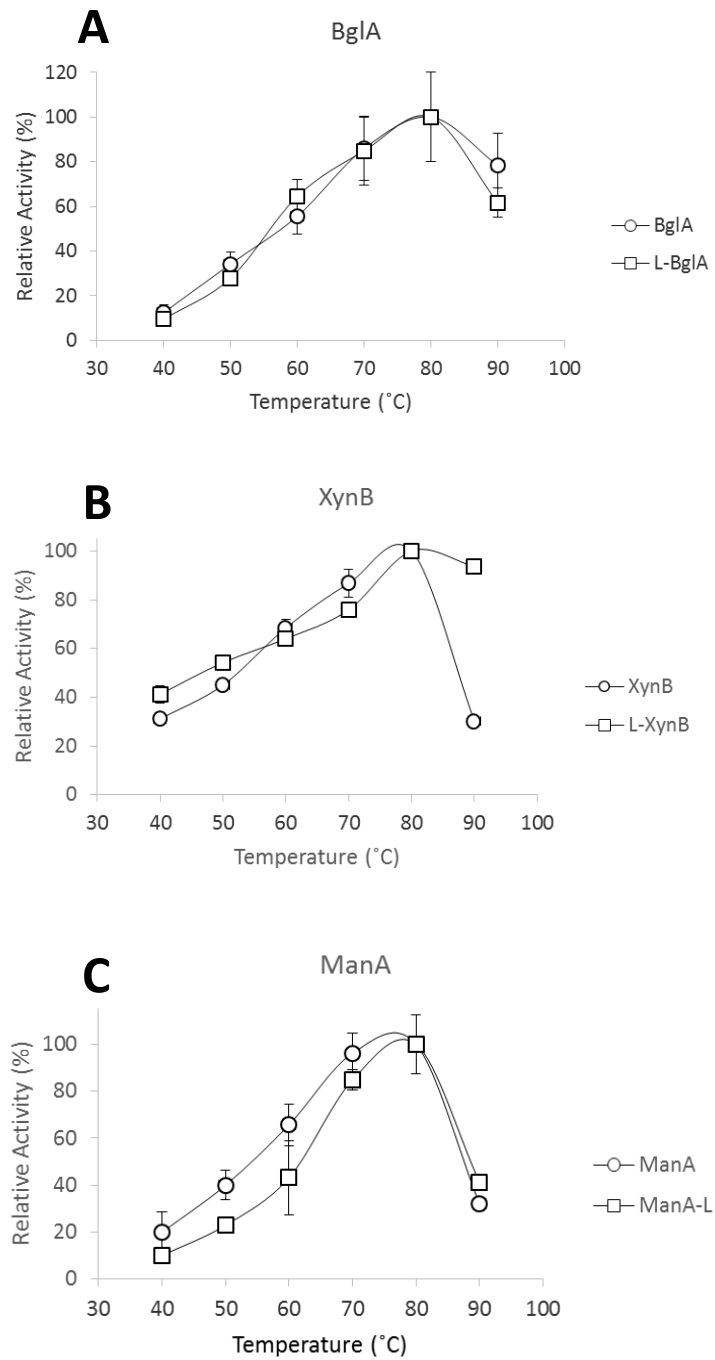


Figure 3-2: Optimal temperatures for activity of free enzymes with (L-BglA, L-XynB and ManA-L) and without (BglA, XynB and ManA) the Linker peptide. (A) BglA and L-BglA, (B) XynB and L-XynB, (C) ManA and ManA-L.

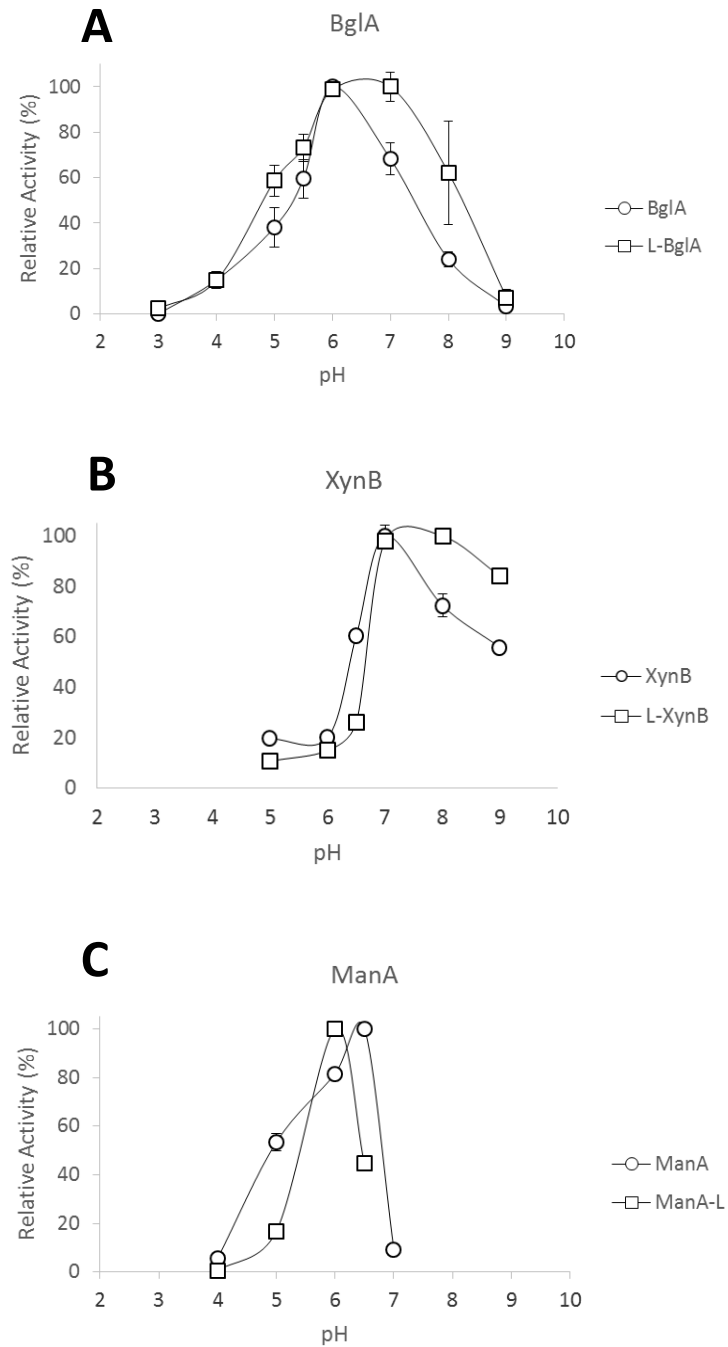


Figure 3-3: Optimal pH's for activity of free enzymes with and without the Linker peptide. BglA and L-BglA display highest relative activity at pH 6.0. XynB and L-XynB display highest relative activity at pH 7.0, and ManA and ManA-L display highest relative activity at pH 6.5 and pH 6.0, respectively. (A) BglA and L-BglA, (B) XynB and L-XynB, (C) ManA and ManA-L.

## Enzyme immobilisation

### *Zeolite-bound enzymes (zeo-enzyme)*

Standard zeolite binding assays were performed with partially purified enzymes (with and without the Linker, Figure 3-4). All enzymes carrying the Linker (L-BglA, L-XynB and ManA-L) displayed strong binding affinity for the zeolite matrix with approximately 100% of their initial protein found in the final zeolite-bound fraction. Enzymes without the Linker (BglA, XynB and ManA) displayed no binding affinity to the zeolite matrix. Almost all of their initial protein was found in the unbound fractions with minimal protein present in the first wash fraction.

These results indicated that introduction of the Linker sequence into the three thermostable enzymes did not have any negative effects on the zeolite binding affinity of the Linker. Furthermore, the position of the Linker (N- or C-terminus) with respect to the enzyme sequence did not affect its zeolite binding function.

Zeo-enzymes were synthesised using standard binding assays of partially purified Linker-enzymes without the final SDS heat elution step. All enzymes carrying the Linker (L-BglA, L-XynB and ManA-L) displayed strong binding affinity for the zeolite matrix. The zeolite-bound fraction retained activity similar to that of the free enzymes, while negligible activity was found in any of the other assay fractions (results not shown). Enzymes without the Linker (BglA, XynB and ManA) displayed no binding affinity to the zeolite matrix. Almost all of their activity was found in the unbound fractions with minimal activity present in the first wash fraction and zeolite-bound fraction.

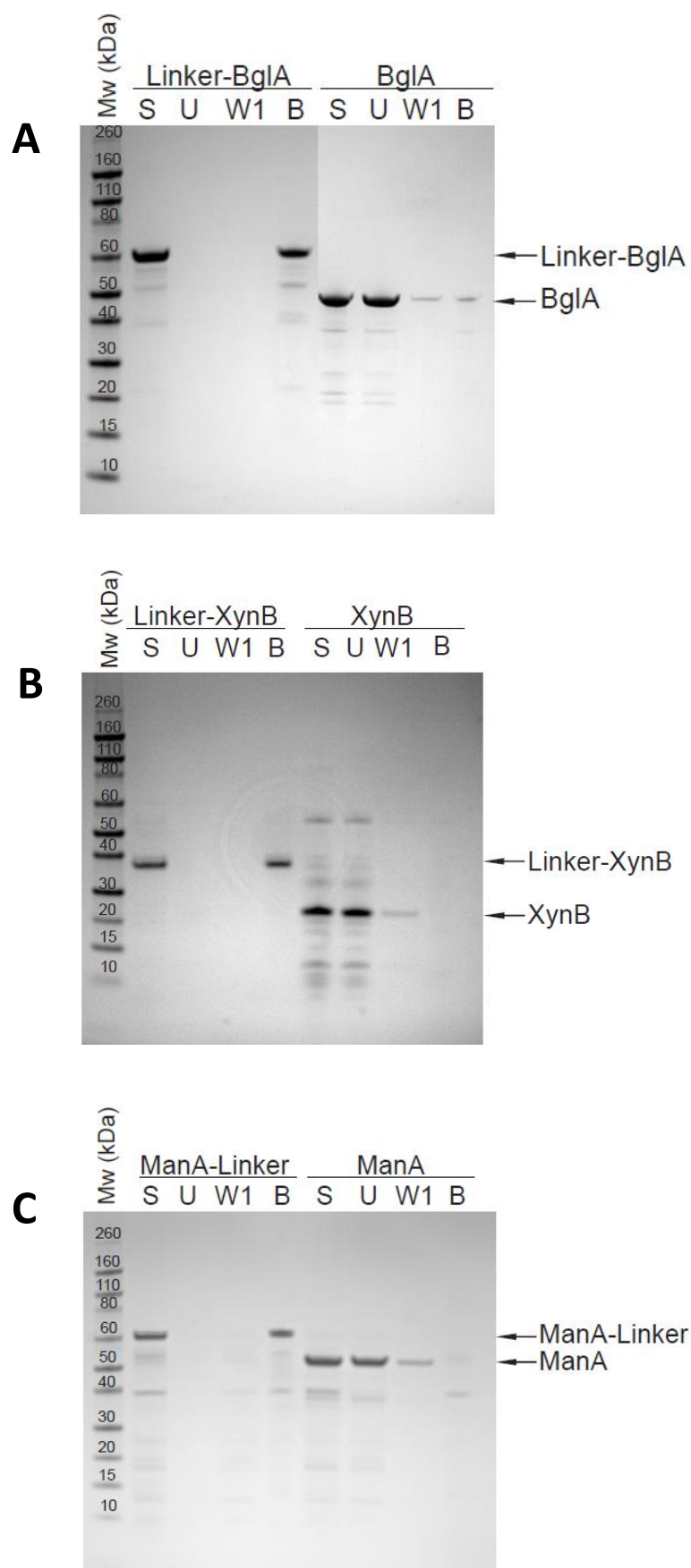


Figure 3-4: Binding assays of thermostable enzymes with and without the Linker peptide. Linker-enzymes (L-BglA, L-XynB and ManA-L) displayed high binding affinity towards the zeolite matrix with most of the initial protein remaining bound to the matrix. In the absence of the Linker, most of the initial enzymes (BglA, XynB and ManA) are found in the unbound fraction. (A) BglA and L-BglA, (B) XynB and L-XynB, (C) ManA and ManA-L; S; starting protein, U; unbound protein, W1; wash fraction (three washing steps, only one shown), B; bound protein fraction.

#### *CLEAs of free enzymes (enzyme<sub>CLEAs</sub>)*

CLEAs of the free enzymes were synthesised using ethanol precipitation and cross-linking at 4°C. Several precipitants were tested, including ammonium sulfate and isopropanol, but ethanol gave the most rapid and complete precipitation. Allowing the cross-linking reaction to proceed overnight without shaking gave the best results in terms of residual activity left in the supernatant and in the resulting activity of the CLEA pellet.

#### *CLEAs of zeolite-bound enzymes (zeo-L-enzyme<sub>CLEAs</sub>)*

It is to be expected that as the concentration of glutaraldehyde in the zeo-L-enzyme<sub>CLEAs</sub> increases, so do the sizes of the CLEAs formed as a result. To test this notion, scanning electron microscopy (SEM) on the zeo-L-BglA<sub>CLEA</sub> samples exposed to different glutaraldehyde concentrations was done using a JEOL-SM-6480 scanning electron microscope (Figure 3-5). The images showed that particle sizes increase as the concentration of glutaraldehyde increases. Zeo-L-BglA<sub>CLEA</sub> particles are ~2.5µm long (Figure 3-5A), 0.5% glutaraldehyde particles are ~15µm long (Figure 3-5B), 3% glutaraldehyde particles are ~20µm long (Figure 3-5C), and 10% glutaraldehyde particles are ~40µm long (Figure 3-5D).



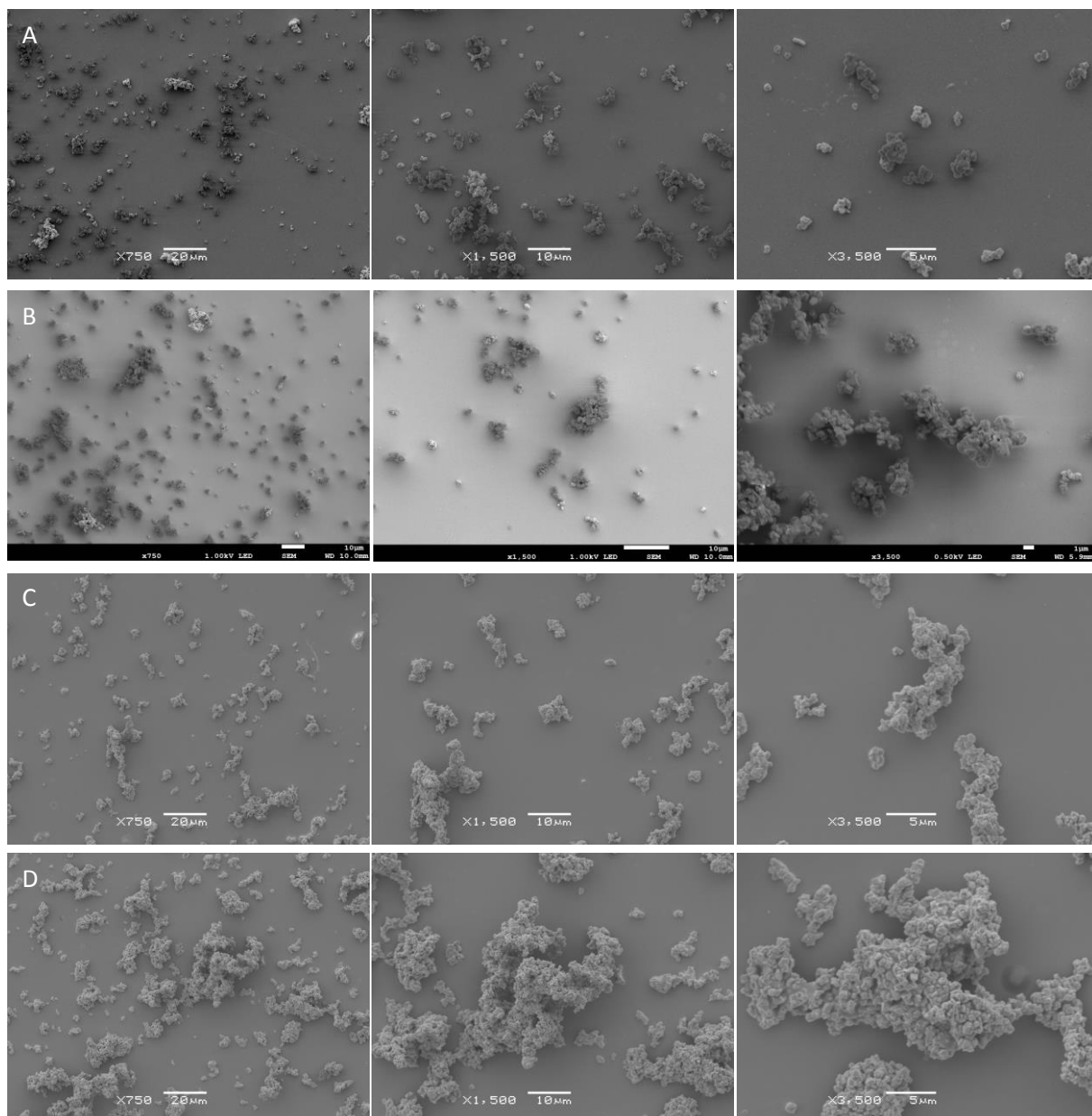


Figure 3-5: Scanning electron microscopy images of L-BglA zeo-CLEAs. Three images of each sample were taken: 750x, 1500x, and 3500x. The B series of images were taken using a FESEM (field emission scanning electron microscope), which can operate at lower voltages than a standard SEM to reduce charging, image artefacts that occur when negative charges build up on a specimen. This phenomenon occurs due to a specimen that is not properly electrically grounded, a problem with the smaller particles. All other images were taken at 5kV. A; non-cross-linked control, B; 0.5% glutaraldehyde, C; 3% glutaraldehyde, D; 10% glutaraldehyde.

The cross-linking reaction was verified by elution of Linker-enzymes from the matrix before activity characterisation of zeo-L-enzyme<sub>CLEAs</sub> was examined. Two different elution buffers (betaine, 1M, pH 6.0 and L-arginine, 1M, pH 6.0) known to elute the Linker peptide from zeolite were tested to determine whether or not Linker-enzymes retain their corresponding enzymatic activity when they are used as elution buffers (Figure 3-6).

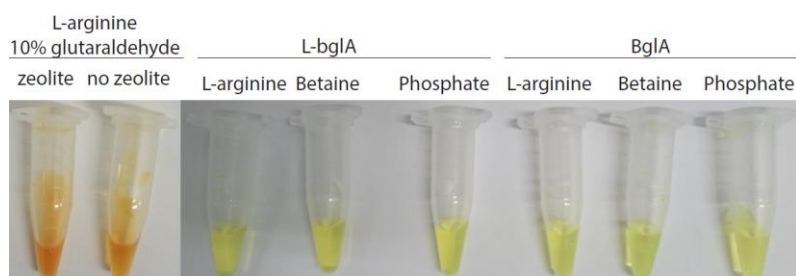


Figure 3-6: Elution buffer tests of 1M betaine and 1M L-arginine. Both buffers are known to elute the Linker from zeolite, but it was unknown whether L-BglA and BglA activity would remain in these buffers. Using substrate at 0.5mg/mL, it was shown that L-BglA and BglA retain activity in both buffers. However, a reaction between L-arginine and glutaraldehyde produces the orange colour independently of the presence of enzyme seen in the two tubes on the left. Phosphate buffer was used as a control.

Betaine (1M, pH 6.0) was determined as the most suitable elution buffer for all enzymes. A successful cross-linking reaction should prevent elution of Linker-enzymes from the zeolite through the strength of the covalent bonds between the enzyme molecules. Three different glutaraldehyde concentrations were tested using L-BglA. After the zeo-L-enzyme<sub>CLEAs</sub> were washed with phosphate buffer, 100µL of 1M betaine was added and incubated at room temperature for 5 minutes with rotation. This step was repeated three times to allow for enzyme elution.

The undesirable side reaction of L-arginine with glutaraldehyde means that L-arginine should not be used to elute the Linker from any CLEAs that have been made with glutaraldehyde as the cross-linking reagent. The cross-linking reaction involves glutaraldehyde reacting with arginine and lysine residues, which may explain the side reaction with the L-arginine buffer.

Standard activity assays were run on all assay fractions and the fractions that displayed activity are shown in Figure 3-7. The relative activity of each fraction is calculated as a percentage of the starting material. All the activity of the 10% glutaraldehyde CLEAs was retained in the CLEAs fraction and

none was present in the elution fractions. Accordingly, 10% (v/v) glutaraldehyde was used for all further cross-linking reactions (including CLEAs from ethanol-precipitated free enzymes). CLEAs prepared with the lower concentrations of glutaraldehyde, 0.5% and 3%, displayed residual enzyme activities of 55% and 20% less than the 10% glutaraldehyde CLEAs fraction. The remaining activity of the lower glutaraldehyde concentrations was found in the elution fractions. This result indicated that at 0.5% and 3% glutaraldehyde, linker-enzymes were not being cross-linked by glutaraldehyde and were consequently being eluted from the zeo-L-enzyme<sub>CLEAs</sub>. One glutaraldehyde molecule is able to form a covalent bond between one lysine and one arginine residue. An excess of glutaraldehyde should be present in order for cross-linking to proceed to a suitable degree.

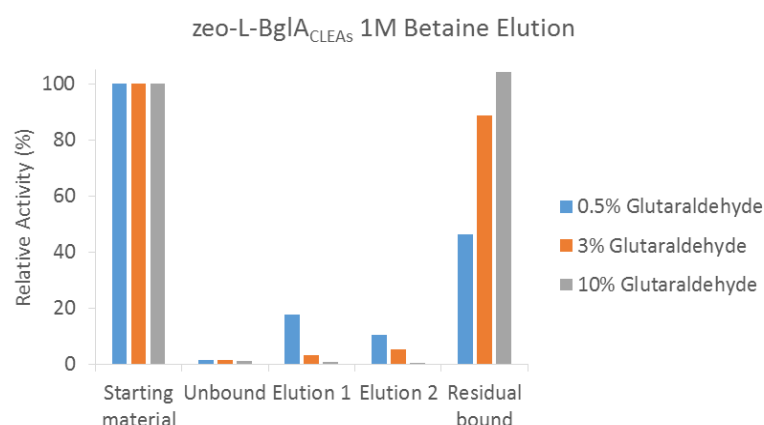


Figure 3-7: Activity profiles of zeo-L-BglA<sub>CLEAs</sub> eluted from the zeolite using 1M betaine. Three different concentrations of glutaraldehyde were used for cross-linking. Activity is measured relative to the starting material (free L-BglA). The unbound fraction was assayed prior to cross-linking, the elution fractions assayed after cross-linking and elution with 1M betaine, and the residual bound fraction was assayed after cross-linking, elution with 1M betaine, and elution with 1x SDS.

The process was repeated with L-XynB and ManA-L once 10% glutaraldehyde was established as the most suitable glutaraldehyde concentration for cross-linking. Activity assays also were done on all fractions (results not shown) and protein bands displaying activity were visualised using SDS-PAGE, along with control zeo-enzymes that also underwent 1M betaine elution (Figure 3-8). Protein bands can be seen in the elution 1 and elution 2 fractions of the zeo-enzymes, where there are none in the elution fractions of the zeo-L-enzyme<sub>CLEAs</sub>. Protein can be seen in the residual bound fractions of the zeo-enzymes, while no residual bound protein can be seen in the zeo-L-enzyme<sub>CLEAs</sub>, despite the activity found in the residual zeolite-bound fractions, presumably because the concentration was below the detection limit of Coomassie Brilliant Blue.

Mixed zeo-enzymes with and without the Linker were synthesised in preparation for multiple substrate hydrolysis using all enzymes to check that multiple enzyme immobilisation onto zeolite was possible. Two standard binding assays were carried out using 100µL of each partially purified enzyme and Linker-enzyme and visualised on SDS-PAGE. After confirmation that all three Linker-enzymes were successfully immobilised (Figure 3-9), cross-linking validation and activity characterisation of zeo-L-enzyme<sub>CLEAS</sub> was carried out. The three Linker-enzymes retained affinity for silica-containing materials when immobilised onto the same matrix. Enzymes without the Linker displayed very low affinity with most of the protein in the unbound fraction. Unfortunately, BglA and ManA are both 50kDa, and appear as a single band upon SDS-PAGE visualisation, as do L-BglA and ManA-L. However, the combined band appears at approximately twice the intensity of the XynB band.

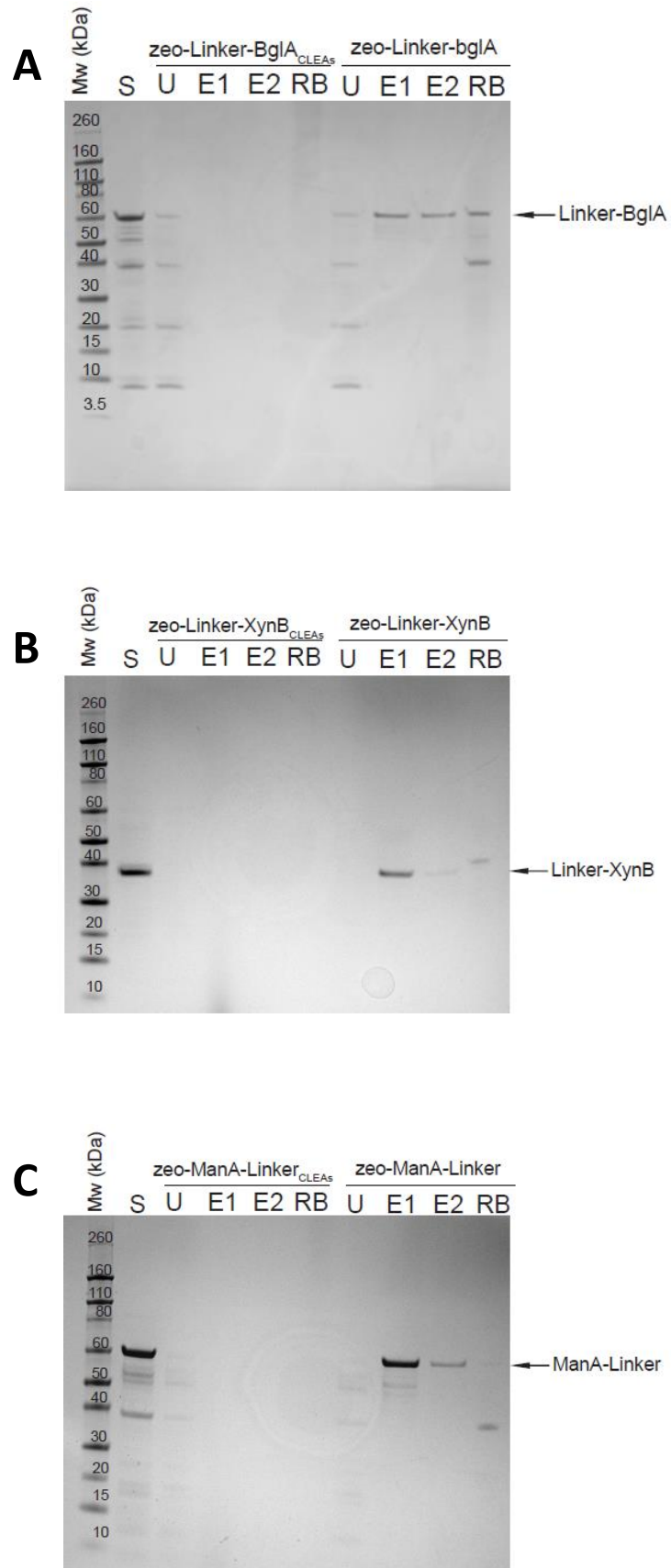


Figure 3-8: 1M betaine elution of zeo-L-enzyme<sub>CLEAs</sub> and zeo-L-enzymes. After cross-linking, incubation with 1M betaine does not elute any protein from the zeo-L-enzyme<sub>CLEAs</sub>, while protein was eluted from the zeo-L-enzymes. A small amount of protein remained in the residual bound fraction of the zeo-L-enzymes, while none was seen in the residual bound fraction of the zeo-L-enzyme<sub>CLEAs</sub>. S; starting protein, U; unbound protein, E1; elution fraction 1, E2; elution fraction 2, RB; residual bound.

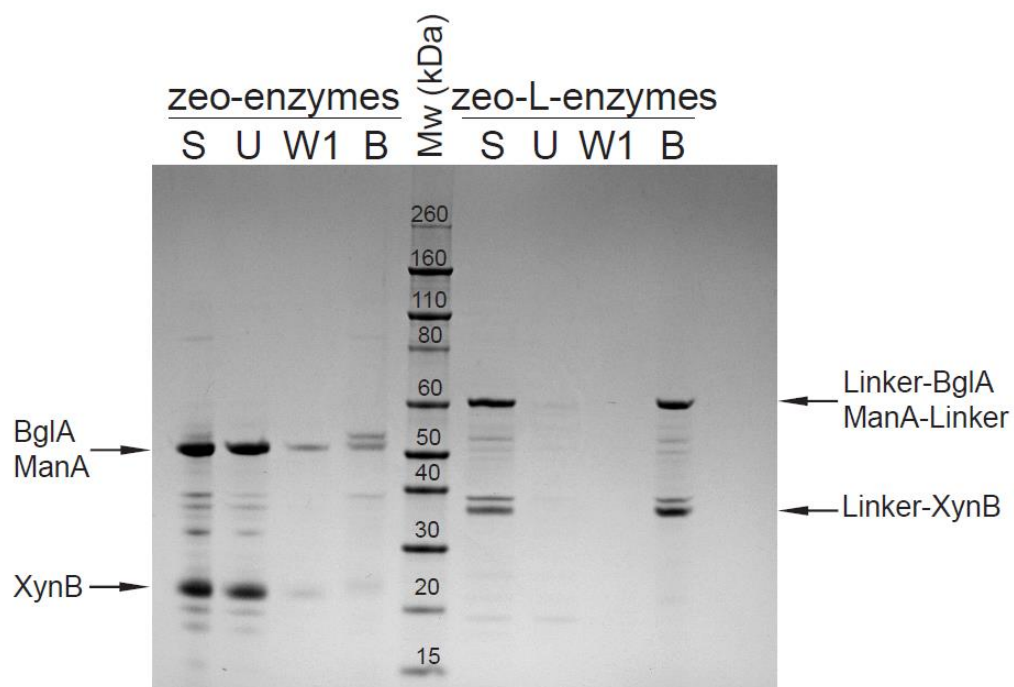


Figure 3-9: Binding assay of mixed zeo-enzymes with and without the silica-binding Linker peptide. All three Linker-enzymes display the same high binding affinity towards silica-containing materials seen in single binding assays with most of the initial protein remaining in the bound fraction. In the absence of the Linker, most of the initial enzymes were found in the unbound fraction. BglA and ManA are both 50 kDa in size, so they appeared as a band approximately twice the intensity of XynB. S; starting protein, U; unbound protein, W1; wash fraction (three steps, only one shown), B; bound protein fraction.

## Activity characterisation of immobilised enzymes

All zeo-L-enzyme<sub>CLEAs</sub> were active between 40°C and 90°C with optimal activity at 80°C (Figure 3-10). The cross-linking of the zeolite-bound enzymes had no effect on the optimal temperature compared to both the free enzymes and the enzyme<sub>CLEAs</sub>. No change in the overall activity profile over the temperatures tested was observed with zeo-L-BglA<sub>CLEAs</sub>, L-BglA<sub>CLEAs</sub> and BglA<sub>CLEAs</sub> (Figure 3-10A), and zeo-ManA-L<sub>CLEAs</sub>, ManA-L<sub>CLEAs</sub>, and ManA<sub>CLEAs</sub> (Figure 3-10C). However, zeo-L-XynB<sub>CLEAs</sub> displayed 50% more activity at 90°C than L-XynB<sub>CLEAs</sub> (Figure 3-10B).

Zeo-L-BglA<sub>CLEAs</sub> were active from pH 3.0 to pH 9.0, with optimum activity at pH 5.0 (Figure 3-11) and the zeo-L-BglA<sub>CLEAs</sub> showed a broader activity range than the BglA<sub>CLEAs</sub> with and without the Linker. A 'shoulder' (a secondary smaller peak that deviates from the smooth curve trend) can be seen in the L-BglA<sub>CLEAs</sub> curve that is not present in the BglA<sub>CLEAs</sub>. Zeo-L-XynB<sub>CLEAs</sub> are active from pH 4.0 to pH 9.0, with optimal activity at pH 6.0. The zeo-L-XynB<sub>CLEAs</sub> showed a broader activity range than the XynB<sub>CLEAs</sub>, but does not show the activity retention at pH 8.0 and 9.0 seen with L-XynB<sub>CLEAs</sub> and free enzymes (Figure 3-11B). L-XynB<sub>CLEAs</sub> and free L-XynB retain 80% activity at pH 8.0 and 9.0, compared to 40% activity of zeo-L-XynB<sub>CLEAs</sub> at the same pH values. Zeo-ManA-L<sub>CLEAs</sub> were active from pH 5.0 to pH 7.0, with optimal activity at pH 6.5. No other change in the overall activity profile over the pH values tested was observed between zeo-ManA-L<sub>CLEAs</sub> and ManA<sub>CLEAs</sub> with and without the Linker (Figure 3-11C).

All enzyme<sub>CLEAs</sub> with and without the Linker were active from 40°C to 90°C, with optimal activity at 80°C. Cross-linking free enzymes did not change the optimal temperature from that of the free enzymes (Figure 3-10). L-enzyme<sub>CLEAs</sub> were generally more active at each temperature tested than the enzyme<sub>CLEAs</sub> without the Linker. The 'shoulder' is present again between pH 5.0 and 6.0 in all BglA<sub>CLEAs</sub>, (Figure 3-11A). However, L-BglA<sub>CLEAs</sub> displayed the same activity as BglA<sub>CLEAs</sub> at 90°C.

All enzyme<sub>CLEAs</sub> show greater variation in optimum pH than the corresponding free enzymes (Figure 3-11). BglA<sub>CLEAs</sub> with and without the Linker were active from pH 3.0 to pH 9.0, with optimal activity at pH 6.0 and 7.0, respectively. The 'shoulder' seen in the BglA<sub>CLEAs</sub> curves is seen again between pH 5 and pH 6, where activity deviated from the curve trend (Figure 3-11A). XynB<sub>CLEAs</sub> with and without the Linker were active from pH 5.0 to pH 9.0, and were both optimally active at pH 6.5. L-XynB<sub>CLEAs</sub>

displayed 70% more activity at pH 9.0 than XynB<sub>CLEAs</sub> (Figure 3-11B). ManA<sub>CLEAs</sub> with and without the Linker were active from pH 5.0 to pH 7.0, and were optimally active at pH 6.0. No change in the overall activity profile over the pH values tested was observed with ManA<sub>CLEAs</sub> and ManA-L<sub>CLEAs</sub> (Figure 3-11C).

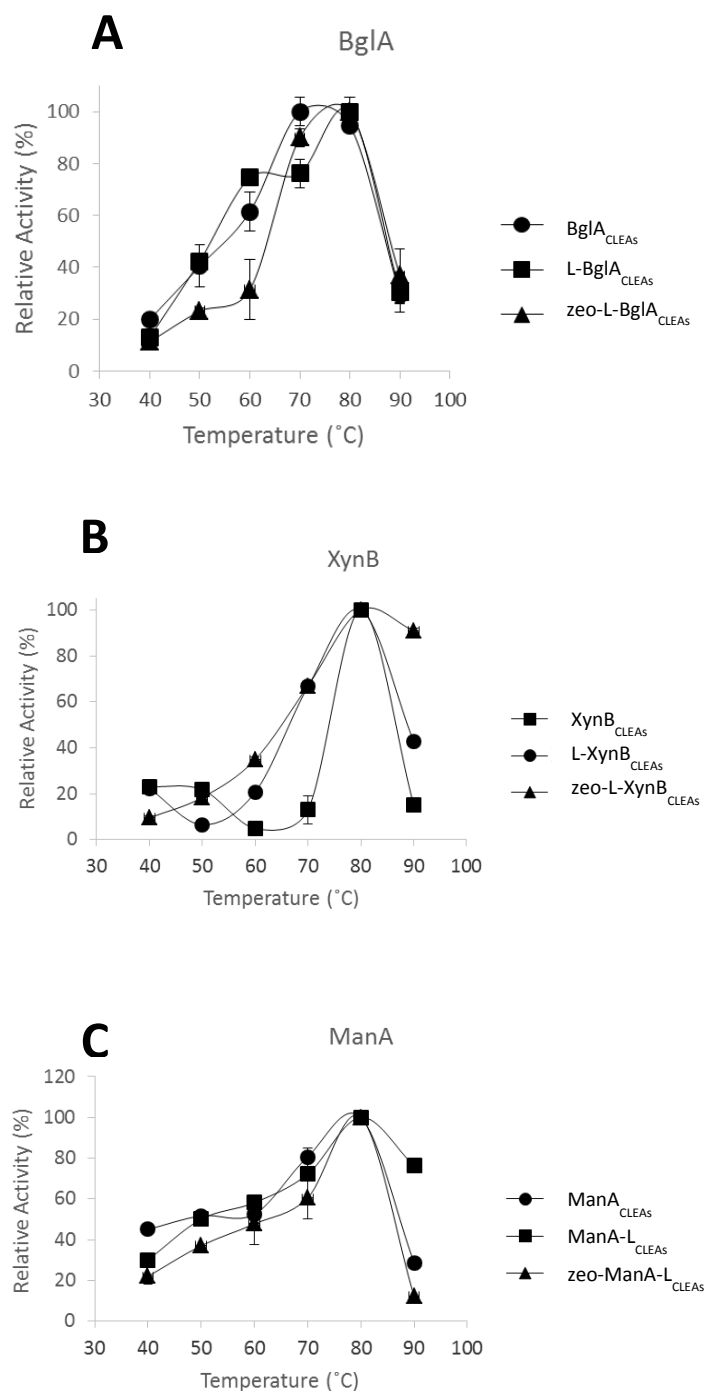


Figure 3-10: Optimal temperature curves of all enzyme CLEAs. All forms of enzyme CLEAs display optimal activity at the same temperature (80°C). A; BglA<sub>CLEAs</sub> with and without the Linker, B; XynB<sub>CLEAs</sub> with and without the Linker, C; ManA<sub>CLEAs</sub> with and without the Linker.



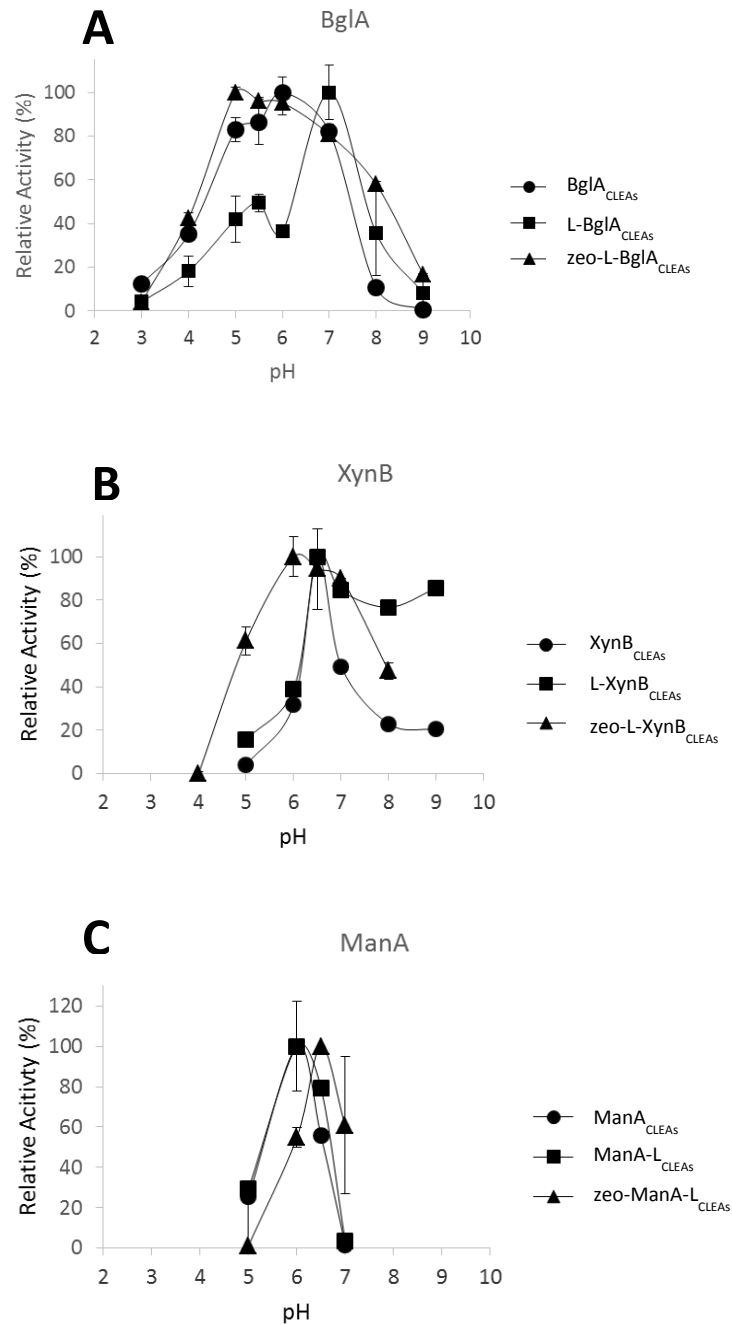


Figure 3-11: Optimal pH curves of all enzyme CLEAs. BglA<sub>CLEAs</sub> displayed optimal activity at pH 6, L-BglA<sub>CLEAs</sub> display optimum activity at pH 7, and zeo-L-BglA<sub>CLEAs</sub> displayed optimum activity at pH 5.0, as well as the broadest pH curve. XynB<sub>CLEAs</sub> and L-XynB<sub>CLEAs</sub> showed optimal activity at pH 6.5, while zeo-L-XynB<sub>CLEAs</sub> showed optimum activity at pH 6, as well as the broadest curve. ManA-L<sub>CLEAs</sub> and ManA<sub>CLEAs</sub> both display optimal activity at pH 6, while zeo-ManA-L<sub>CLEAs</sub> displayed optimal activity at pH 6.5. A; BglA/L-BglA CLEAs, B; XynB/L-XynB CLEAs, C; ManA/ManA-L CLEAs.

## Recycling immobilised enzymes

Recycling assays were carried out on all immobilised enzyme forms (zeo-L-enzyme<sub>CLEAs</sub>, enzyme<sub>CLEAs</sub> and zeo-enzymes) to determine the degree to which different immobilisation methods improve activity retention during enzyme recycling (Figure 3-12). After 12 uses of 10 minutes each, zeo-L-enzyme<sub>CLEAs</sub> retained the most activity, losing between 40% and 60% of their initial activity. They were followed by zeo-enzymes and L-enzyme<sub>CLEAs</sub>, which showed approximately equal activity retention rates, losing between 50% and 80% of their initial activity. Enzyme<sub>CLEAs</sub> showed the worst activity retention rates overall, losing between 70% and 90% of their initial activity. These results were consistent across BglA, XynB and ManA. BglA with and without the Linker consistently showed the best activity retention across all enzyme forms compared to ManA and XynB with and without the Linker. BglA<sub>CLEAs</sub> without the Linker showed marked activity retention compared to the other two enzyme<sub>CLEAs</sub> without the Linker, as after one use, the activity of XynB<sub>CLEAs</sub> and ManA<sub>CLEAs</sub> lost 80% activity compared to BglA<sub>CLEAs</sub>, which lost 15% activity. These results indicated that a combination of zeolite binding and cross-linking was the most effective method with which to immobilise these thermostable enzymes, as they provided greater activity retention than enzymes immobilised with the two methods separately.

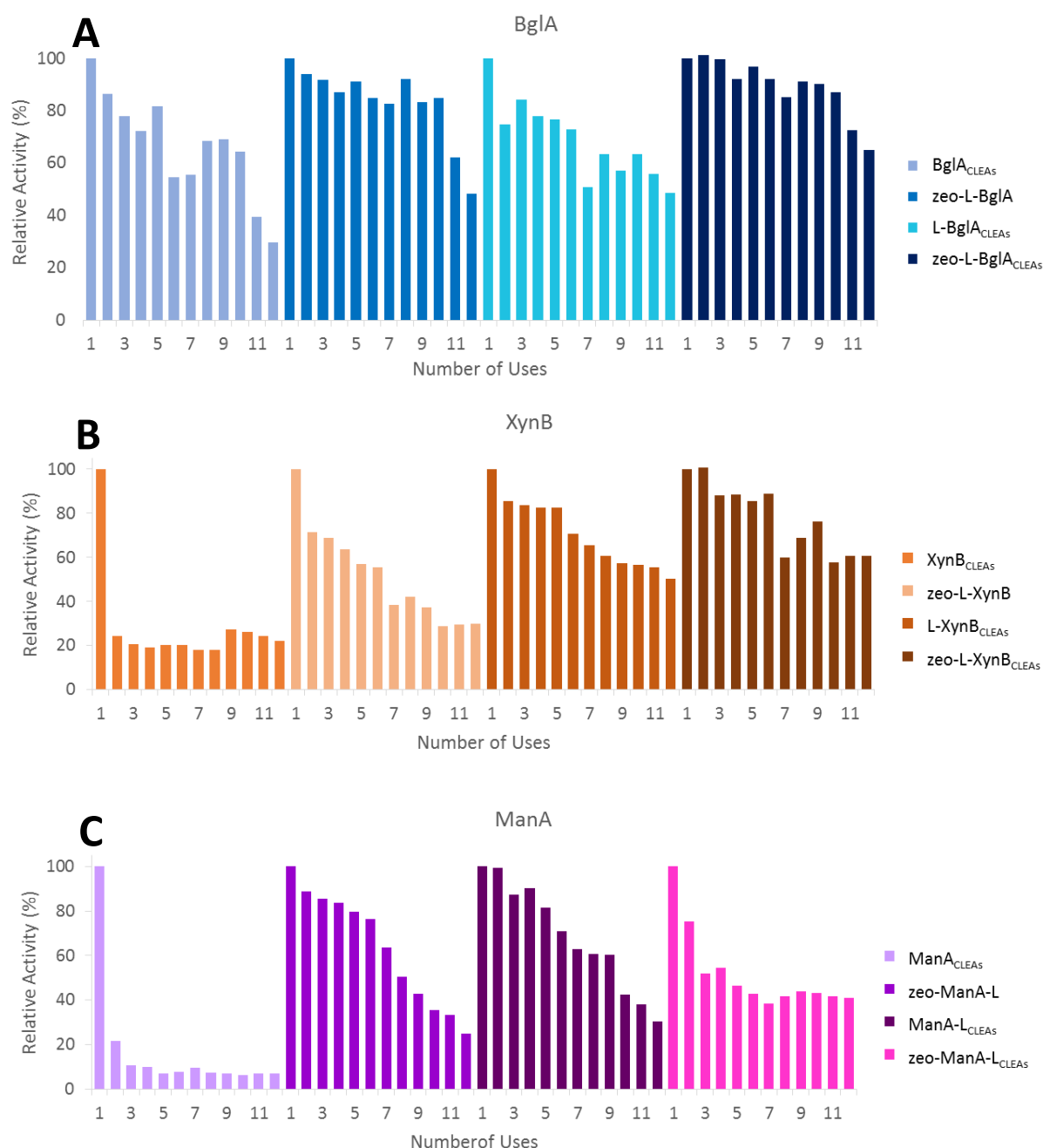


Figure 3-12: Reuse of all forms of immobilised enzymes. Enzyme<sub>CLEAs</sub> showed the lowest activity retention after 12 uses, dropping to 10-30% of initial activity following 12 uses. Zeo-enzymes and L-enzyme<sub>CLEAs</sub> showed comparable activity retention levels after 12 uses, dropping to between 20-50% of initial activity. Zeo-L-enzyme<sub>CLEAs</sub> showed the highest rate of activity retention across all enzymes, retaining between 40-60% of initial activity after 12 uses.

## Multiple substrate hydrolysis

Mixed zeo-L-enzyme<sub>CLEAs</sub> were synthesised and their activity compared to single zeo-L-enzyme<sub>CLEAs</sub>. Activity of the mixed zeo-L-enzyme<sub>CLEAs</sub> for each substrate was measured as a percentage of activity of the corresponding single zeo-L-enzyme<sub>CLEA</sub>. The mixed zeo-L-enzyme<sub>CLEAs</sub> showed activity against all three substrates (Table 3-1). Single zeo-L-enzyme<sub>CLEAs</sub> also were tested against all three substrates and no single zeo-L-enzyme<sub>CLEA</sub> showed activity against any other substrate except that of its constituent enzyme. The activity of the mixed zeo-L-enzyme<sub>CLEAs</sub> was generally less than the activity of the single zeo-L-enzyme<sub>CLEAs</sub>. The exception was L-BglA, which retained 98% of the activity of the single zeo-L-BglA<sub>CLEAs</sub>.

Table 3-1: Activity of mixed zeo-L-enzyme<sub>CLEAs</sub>, measured as a percentage of the activity of the single zeo-enzyme<sub>CLEAs</sub>. The individual reactions carried out by the mixed zeo-L-enzyme<sub>CLEAs</sub> showed less activity than the single zeo-enzyme<sub>CLEAs</sub> carrying out the same reaction. However, no single zeo-L-enzyme<sub>CLEA</sub> showed activity against more than one substrate.

		zeo-L-enzyme <sub>CLEAs</sub> Relative Activity (%)			
		L-BglA	L-XynB	ManA-L	L-BglA L-XynB ManA-L
Substrate	pNPGluc	100	0.80	0.83	98.75
	OSX	0.62	100	0.40	56.32
	LBG	8.35	0.36	100	41.39

## Chapter 4 Discussion

We have genetically fused a silica-binding Linker peptide to three thermostable polysaccharide-degrading enzymes for applications in industrial-scale biocatalysis. The Linker peptide showed high affinity for silica-containing support materials, allowing for directional immobilisation of the three enzymes onto a zeolite. The partially-purified fusion proteins retained both biological activity and binding affinity for zeolite. This was independent of the position of the Linker (N- or C-terminal). ManA-L displayed strong silica-binding activity comparable to L-BglA and L-XynB and in contrast to ManA, even though the Linker was C-terminal to ManA, and N-terminal to BglA and XynB.

The addition of the Linker had no negative effects on the pH and temperature stability of the enzymes. The Linker peptide did not appear to affect optimum temperature for activity of any of the free enzymes, but appeared to have an effect on the pH, seen in L-BglA and L-XynB. The presence of the Linker on ManA caused a shift in the optimum pH.

No protein was seen in the 1M betaine elution fractions of the zeo-L-enzyme<sub>CLEAs</sub>, indicating that the cross-linking was effective and no enzyme leakage was observed. The absence of residual bound protein in the SDS-PAGE visualisation of the zeo-L-enzyme<sub>CLEAs</sub> can be attributed to SDS failing to elute the enzymes due to the presence of the covalent bonds. Additionally, it seems that 0.5% and 3% glutaraldehyde concentrations are not sufficient for the cross-linking reaction to proceed to completion, as evidenced by the activity seen in the elution fractions in Figure 3-7. However, our optimisation showed that 10% glutaraldehyde is the most effective concentration for immobilisation. The values of 0.5% and 3% were chosen as the lowest and highest concentrations of glutaraldehyde used for cross-linking found in literature [72].

Cross-linking enzymes to create CLEAs appears to have stabilised the activity with respect to pH, as the CLEAs of BglA and XynB show higher activity at sub-optimal pH values than the free enzymes. At pH 6.0, one pH unit from the optimum, zeo-L-BglA<sub>CLEAs</sub> retained 90% activity, while BglA at one pH unit from its optimum retained 60% activity. Similarly, zeo-L-XynB<sub>CLEAs</sub> retained 80% activity at one pH unit from the optimum, while XynB activity falls to 60% one pH unit from its optimum. The stabilising effect is present with respect to temperature too, but to a lesser degree than the pH effect. Overall,

this stabilisation effect is more pronounced with the zeo-L-enzyme<sub>CLEAs</sub> than with the enzyme<sub>CLEAs</sub> with and without Linkers.

Previous research comparing CLEAs to native enzymes has shown that enzyme cross-linking broadens the pH values at which the enzyme is active, as well as increasing total activity in U/g/mL [73]. CLEAs were also shown to increase the temperature range at which the enzyme was active [73]. The broadening of activity ranges seen in CLEAs is due to the stabilising nature of the cross-linking reaction. When the enzymes are cross-linked, they are in their native form, and the covalent bonds of the cross-linking reaction protect the enzyme from any tertiary structure distortion caused by heat. This is further evidenced by the lack of optimum temperature broadening seen in the free enzymes between the Linker and non-Linker enzymes, indicating that it is the cross-linking and not the presence of the Linker peptide that is responsible for the increased activity range at sub-optimal pH and temperature conditions.

The deviation from the curve trend (a secondary smaller peak, referred to as a 'shoulder') seen in the L-BglA<sub>CLEA</sub> temperature and pH measurements (present at 60°C and pH 5.0, respectively) could be a result of precipitation refolding. Precipitation with organic solvents (such as ethanol) carries a denaturation risk, which would be carried over to the immobilised form when the enzymes were cross-linked [74]. A small portion of the L-BglA may have denatured and then refolded incorrectly, producing the deviation from the curve trend [74]. The same stock of BglA<sub>CLEAs</sub> were used for both temperature and pH measurements, which explains why the shoulder shows up in both measurements.

CLEAs made using enzymes immobilised before cross-linking display higher activity to both free enzymes and CLEAs made from precipitated free enzymes [28]. Previous research has been done on xylanolytic enzymes immobilised onto silanised magnetic particles and cross-linked together. This research showed that in comparison to both free xylanase and precipitated free enzyme CLEAs, the magnetic CLEAs displayed superior thermostability and activity [28].

The ability to recycle enzymes for subsequent uses is an important property in the use of immobilised enzymes in industrial biocatalysis. Unlike free enzymes, immobilised enzymes can be

removed from the reaction medium and used for multiple reactions before being discarded, which cuts down on operating costs and resources spent producing fresh enzymes. It has been shown previously that immobilised enzymes retain significant amounts of activity when substrate is exchanged after a reaction period for fresh substrate and the enzyme is recycled [75]. Recycled immobilised enzymes retain activity for much longer compared to enzyme samples incubated for the same amount of time without the substrate, where activity is tested after the incubation period (thermal inactivation). This phenomenon is known as substrate stabilisation. Binding of the substrate to the active site helps to stabilise the enzyme in its native conformation and protect it from heat denaturation [76].

The zeo-L-enzyme<sub>CLEAs</sub> of all enzymes display the most activity retention (only losing between 30% and 40% initial activity) after twelve 10-minute uses, equivalent to two hours spent at the optimum temperature. The Linker is 23% Lys or Arg residues, which participate in the cross-linking reaction. The stabilisation provided by these extra residues is a possible reason as to why the zeo-L-enzyme<sub>CLEAs</sub> are the most stable over 12 recycling assays. The stabilising effect provided by the Linker could also provide an explanation as to why the enzyme<sub>CLEAs</sub> without Linkers were the least recyclable over all enzymes (losing between 80% and 90% initial activity after 12 uses). Without the extra stabilisation provided by the Linker, the enzyme<sub>CLEAs</sub> would be more prone to denaturation and loss of activity than immobilised enzymes with Linkers.

Zeo-enzymes display better activity retention than the enzyme<sub>CLEAs</sub>, showing between 20% and 30% more activity retention after 12 uses across all three enzymes. However, they show less recyclability than the L-enzyme<sub>CLEAs</sub> with and without zeolite (retaining 10% to 30% more activity than the L-enzyme<sub>CLEAs</sub> after 12 uses). This implies that the cross-linking reaction also plays an important role in stabilising the immobilised enzymes against heat-induced denaturation over subsequent uses.

Aside from recyclability, zeo-L-enzyme<sub>CLEAs</sub> have a number of advantages over enzyme<sub>CLEAs</sub>. Zeolite takes the place of the precipitation step, so no optimisation needs to be done trying to find the most suitable cross-linking reagent. There are a large number of precipitation reagents available [77], and determining which precipitation reagent is the most suitable for the protein at hand through sequence methods is unreliable, both in terms of yield and activity retention [74]. Mixed zeo-L-

enzyme<sub>CLEAs</sub> are also easier to make than mixed enzyme<sub>CLEAs</sub>, as mixed enzyme<sub>CLEAs</sub> would require optimisation of precipitation protocols for multiple enzymes. The replacement of the aggregation step also means that there is no denaturation risk to the enzymes. Due to the orientated immobilisation provided by the Linker, the enzymes in the zeo-L-enzyme<sub>CLEAs</sub> are more likely to face out into the reaction medium, providing higher activity levels than enzyme<sub>CLEAs</sub>.

Each of the single zeo-L-enzyme<sub>CLEAs</sub> shows activity against the substrate of the constituent enzyme and negligible activity towards the other two substrates. In contrast, the mixed zeo-L-enzyme<sub>CLEAs</sub> show activity towards all three substrates at approximately half the relative activity of the single zeo-L-enzyme<sub>CLEAs</sub>. Multiple enzyme immobilisation onto silica-based materials has been explored using a technique known as layer-by-layer polyelectrolyte fabrication, where layer deposition of polyelectrolytes is used to coat the charged support with alternating ionic layers. A glucose oxidase and a horseradish peroxidase were immobilised at pH values below their pI values, adsorbing via electrostatic interactions between anionic residues and cationic polyelectrolyte layers deposited onto silica microparticles [78]. Two different structures were synthesised in which glucose oxidase and horseradish peroxidase were immobilised in the same polyelectrolyte layer, and in different ones (Figure 4-1). Regardless of structure, it was found that co-immobilisation of these two enzymes enhanced kinetic activity compared to a mixture of free enzymes [78].

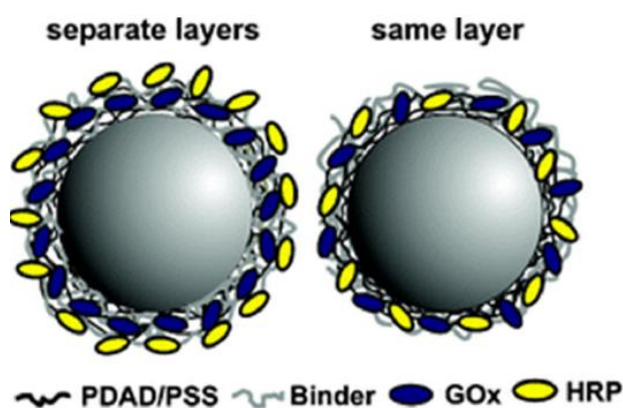


Figure 4-1: Multiple enzyme immobilisation in two different conformations using alternating anionic and cationic polyelectrolytes [62]. PDAD/PSS; anionic poly(diallyldimethylammonium chloride)/poly(sodium 4-styrenesulfonate), Binder; cationic pyridinium-*N*-ethylamine, GOx; glucose oxidase, HRP; horseradish peroxidase.



We have shown that it is possible for multiple thermostable polysaccharide-degrading enzymes to be immobilised onto the same support and retain specific hydrolytic activity. Cross-linking previously immobilised zeo-enzymes is the immobilisation method that shows the most potential for industrial applications. The zeo-L-enzyme<sub>CLEAs</sub> have comparable activity to the free enzymes and superior activity to the enzyme<sub>CLEAs</sub>, with the added bonus of being the most recyclable (i.e. retaining the most activity after multiple reactions) and being the simplest and quickest to synthesise and the easiest to remove from the reaction mixture. This may have implications in the enzymatic breakdown of lignocellulosic substrates for industrial purposes, as well as wider implications in further enzyme immobilisation for production of industrially useful biomolecules.

We selected three thermostable glycoside-hydrolysing enzymes as our model system because there is sufficient published data to allow us to compare the performance of our system against those studies reported previously [65, 67, 79, 80]. Immobilisation of polysaccharide-degrading enzymes has significant economic and environmental impacts due to its potential for industrial-scale glucose production from minimally-treated plant biomass. Downstream applications of glucose produced in this way include fermentation for cellulosic biofuels, a renewable resource with a much smaller carbon footprint than both traditional petroleum-based fuels and starch-based biofuels [81]. Additionally, the use of cellulosic materials for biofuel production does not compete with food production, unlike starch-based biofuels [82]. Large-scale industrial operations using enzyme immobilisation on solid matrices combined with enzyme reuse has the potential to reduce operating and product costs as well as improving the yield of a process.

In previous studies, cellulolytic enzymes have been immobilised using gold-coated nanoparticles immobilised on thiolated magnetic silica nanoparticles. Cysteine-tagged cellulases were bound to the gold nanoparticles using thiol-gold chemistry [83]. The activity of immobilised and free cellulases was compared using HPLC. The yields of glucose and cellobiose were found to increase by 179% and 158%, respectively, when using immobilised cellulases compared to the free ones [83]. Stability and activity of the immobilised cellulases remained after four reuses, while the free enzymes dropped to 40% of their previous activity after a single reuse [83].

Plasma immersion ion implantation (PIII) is a covalent technique that reduces the time and amount of steps compared to conventional covalent immobilisation techniques. PIII involves extracting ions from plasma by applying a high voltage DC current which directs the ions to a polymeric substrate covered by a semiconductor wafer. The ions break bonds in the polymer chains and create free radicals that react covalently with the enzyme [84]. However, PIII treatment must be done under vacuum conditions and plasma is created by superheating gas or applying the gas in a strong electromagnetic field. Flat PIII-treated polystyrene was used as a support to immobilise a thermostable  $\beta$ -glucosidase and a commercially-available  $\beta$ -glucosidase [85]. It was found that the thermostable  $\beta$ -glucosidase displayed higher activity when immobilised onto the PIII-treated polystyrene than when adsorbed onto untreated polystyrene [85]. The immobilised thermophilic  $\beta$ -glucosidase also showed 20 times higher activity than the immobilised commercially available  $\beta$ -glucosidase [85]. PIII has also been used to immobilise a thermophilic  $\beta$ -glucosidase on a curved surface. Using plastic polymer granules support treated with PIII, a thermophilic  $\beta$ -glucosidase from *Caldicellulosiruptor saccharolyticus* was immobilised and retained activity for 2 weeks, compared to 6 days with untreated granules [86].

## Conclusion

The above immobilisation technologies are elegant and ideally suited for laboratory experiments but do not translate well into industrial-scale processes. The platform technology outlined in this thesis has the potential for use in industrial-scale catalysis of commercially important biological products. The ease of synthesis and recyclability of the zeo-L-enzyme<sub>CLEAs</sub>, and the robustness and strength of the support and support-enzyme bond make this an ideal method for large-scale biological production. With only minor optimisation (i.e. optimal pH and temperature), this technology has potential applicability to a wide range of enzymes.

Downstream applications of immobilising polysaccharide-degrading enzymes using the Linker-mediated platform technology outlined in this thesis are in the industrial production of glucose from minimally-treated plant biomass. Further work on this project would include the selection and immobilisation of the remaining enzymes of the classical cellulose degradation pathway, suitable thermostable cellulases endoglucanase and exoglucanase. During the cellulose degradation pathway, enzymatic production of cellobiose usually results in product inhibition. Therefore, the postulation of

a cell-free cellulose degradation pathway using industrial biocatalysis containing immobilised endoglucanase and exoglucanase for sequential hydrolysis may help minimise this inhibitory effect.

Further optimisation of cellulose degradation using mixed zeo-L-enzyme<sub>CLEAS</sub> would involve using a complex, natural, non-synthetic substrate to demonstrate activity retention of L-BglA. This would give a better picture of how such a biocatalytic module would function in an industrial setting.

Our system, based on low-cost bulk matrices and a simple immobilisation technology, is a viable alternative that requires further investigation and optimisation before application at the industrial scale. The thermostable enzymes were chosen because they represent a true industrial application with relevance in biomass degradation and biofuel production.

## Chapter 5 References

1. Betancor, L. and H.R. Luckarift, *Bioinspired enzyme encapsulation for biocatalysis*. Trends in Biotechnology, 2008. **26**(10): p. 566-572.
2. Hanefeld, U., L. Gardossi, and E. Magner, *Understanding enzyme immobilisation*. Chemical Society Reviews, 2009. **38**(2): p. 453-468.
3. Brady, D. and J. Jordaan, *Advances in enzyme immobilisation*. Biotechnology Letters, 2009. **31**(11): p. 1639-1650.
4. Mateo, C., et al., *Improvement of enzyme activity, stability and selectivity via immobilization techniques*. Enzyme and Microbial Technology, 2007. **40**(6): p. 1451-1463.
5. Mateo, C., et al., *Glyoxyl agarose: a fully inert and hydrophilic support for immobilization and high stabilization of proteins*. Enzyme and Microbial Technology, 2006. **39**(2): p. 274-280.
6. Sunna, A., F. Chi, and P.L. Bergquist, *A linker peptide with high affinity towards silica-containing materials*. New Biotechnology, 2013. **30**(5): p. 485-492.
7. Hartmann, M. and X. Kostrov, *Immobilization of enzymes on porous silicas—benefits and challenges*. Chemical Society Reviews, 2013. **42**(15): p. 6277-6289.
8. Lee, H., J. Rho, and P.B. Messersmith, *Facile conjugation of biomolecules onto surfaces via mussel adhesive protein inspired coatings*. Advanced Materials, 2009. **21**(4): p. 431-434.
9. Arica, M.Y., et al., *Immobilization of glucoamylase onto spacer-arm attached magnetic poly (methylmethacrylate) microspheres: characterization and application to a continuous flow reactor*. Journal of Molecular Catalysis B: Enzymatic, 2000. **11**(2): p. 127-138.
10. Guisán, J., *Aldehyde-agarose gels as activated supports for immobilization-stabilization of enzymes*. Enzyme and Microbial Technology, 1988. **10**(6): p. 375-382.
11. Cullen, S.P., I.C. Mandel, and P. Gopalan, *Surface-anchored poly (2-vinyl-4, 4-dimethyl azlactone) brushes as templates for enzyme immobilization*. Langmuir, 2008. **24**(23): p. 13701-13709.
12. Howlett, J.R., D.W. Armstrong, and H. Yamazaki, *Carbonyldiimidazole activation of a rayon/polyester cloth for covalent immobilization of proteins*. Biotechnology Techniques, 1991. **5**(5): p. 395-400.
13. Fernandez-Lafuente, R., et al., *Preparation of activated supports containing low pK amino groups. A new tool for protein immobilization via the carboxyl coupling method*. Enzyme and Microbial Technology, 1993. **15**(7): p. 546-550.
14. Wissink, M., et al., *Immobilization of heparin to EDC/NHS-crosslinked collagen. Characterization and in vitro evaluation*. Biomaterials, 2001. **22**(2): p. 151-163.
15. Van Sommeren, A., P. Machielsen, and T. Gribnau, *Comparison of three activated agaroses for use in affinity chromatography: effects on coupling performance and ligand leakage*. Journal of Chromatography A, 1993. **639**(1): p. 23-31.
16. Misra, A. and P. Dwivedi, *Immobilization of oligonucleotides on glass surface using an efficient heterobifunctional reagent through maleimide–thiol combination chemistry*. Analytical Biochemistry, 2007. **369**(2): p. 248-255.
17. Ratner, D.M., et al., *Tools for glycomics: mapping interactions of carbohydrates in biological systems*. ChemBioChem, 2004. **5**(10): p. 1375-1383.
18. Brocklehurst, K., et al., *Covalent chromatography. Preparation of fully active papain from dried papaya latex*. Biochemical Journal, 1973. **133**: p. 573-584.
19. Fernández-Lafuente, R., et al., *Stabilization of multimeric enzymes via immobilization and post-immobilization techniques*. Journal of Molecular Catalysis B: Enzymatic, 1999. **7**(1): p. 181-189.
20. Caruso, F., et al., *Enzyme encapsulation in layer-by-layer engineered polymer multilayer capsules*. Langmuir, 2000. **16**(4): p. 1485-1488.

21. Kim, J., J.W. Grate, and P. Wang, *Nanostructures for enzyme stabilization*. Chemical Engineering Science, 2006. **61**(3): p. 1017-1026.
22. Colletier, J.-P., et al., *Protein encapsulation in liposomes: efficiency depends on interactions between protein and phospholipid bilayer*. BMC Biotechnology, 2002. **2**(1): p. 9.
23. Graff, A., M. Winterhalter, and W. Meier, *Nanoreactors from polymer-stabilized liposomes*. Langmuir, 2001. **17**(3): p. 919-923.
24. Bruns, N. and J.C. Tiller, *Amphiphilic network as nanoreactor for enzymes in organic solvents*. Nano Letters, 2005. **5**(1): p. 45-48.
25. St. Clair, N.L. and M.A. Navia, *Cross-linked enzyme crystals as robust biocatalysts*. Journal of the American Chemical Society, 1992. **114**(18): p. 7314-7316.
26. Sheldon, R., R. Schoevaart, and L. Van Langen, *Cross-linked enzyme aggregates (CLEAs): A novel and versatile method for enzyme immobilization (a review)*. Biocatalysis and Biotransformation, 2005. **23**(3-4): p. 141-147.
27. Cao, L., F. van Rantwijk, and R.A. Sheldon, *Cross-linked enzyme aggregates: a simple and effective method for the immobilization of penicillin acylase*. Organic Letters, 2000. **2**(10): p. 1361-1364.
28. Bhattacharya, A. and B.I. Pletschke, *Magnetic cross-linked enzyme aggregates (CLEAs): a novel concept towards carrier free immobilization of lignocellulolytic enzymes*. Enzyme and Microbial Technology, 2014. **61**: p. 17-27.
29. Care, A., P.L. Bergquist, and A. Sunna, *Solid-binding peptides: smart tools for nanobiotechnology*. Trends in Biotechnology, 2015.
30. Schreiber, F., *Structure and growth of self-assembling monolayers*. Progress in Surface Science, 2000. **65**(5): p. 151-257.
31. Pensa, E., et al., *The chemistry of the sulfur–gold interface: in search of a unified model*. Accounts of Chemical Research, 2012. **45**(8): p. 1183-1192.
32. Hodneland, C.D., et al., *Selective immobilization of proteins to self-assembled monolayers presenting active site-directed capture ligands*. Proceedings of the National Academy of Sciences, 2002. **99**(8): p. 5048-5052.
33. Cetinel, S., et al., *Addressable self-immobilization of lactate dehydrogenase across multiple length scales*. Biotechnology Journal, 2013. **8**(2): p. 262-272.
34. Weinrib, H., et al., *Uniformly immobilizing gold nanorods on a glass substrate*. Journal of Atomic, Molecular, and Optical Physics, 2012. **2012**.
35. Tamerler, C., et al., *Molecular biomimetics: GEPI-based biological routes to technology*. Peptide Science, 2010. **94**(1): p. 78-94.
36. Keefe, A.D., et al., *One-step purification of recombinant proteins using a nanomolar-affinity streptavidin-binding peptide, the SBP-Tag*. Protein Expression and Purification, 2001. **23**(3): p. 440-446.
37. Care, A., et al., *Biofunctionalization of silica-coated magnetic particles mediated by a peptide*. Journal of Nanoparticle Research, 2014. **16**(8): p. 1-9.
38. Kirchner, C., et al., *Cytotoxicity of colloidal CdSe and CdSe/ZnS nanoparticles*. Nano Letters, 2005. **5**(2): p. 331-338.
39. Magrez, A., et al., *Cellular toxicity of carbon-based nanomaterials*. Nano Letters, 2006. **6**(6): p. 1121-1125.
40. Nel, A.E., et al., *Understanding biophysicochemical interactions at the nano–bio interface*. Nature Materials, 2009. **8**(7): p. 543-557.
41. Li, Y. and Y. Huang, *Morphology-controlled synthesis of platinum nanocrystals with specific peptides*. Advanced Materials, 2010. **22**(17): p. 1921-1925.
42. Chiu, C.-Y., et al., *Platinum nanocrystals selectively shaped using facet-specific peptide sequences*. Nature Chemistry, 2011. **3**(5): p. 393-399.

43. Nanda, K., et al., *Higher surface energy of free nanoparticles*. Physical Review Letters, 2003. **91**(10): p. 106102.
44. Coppage, R., et al., *Exploiting localized surface binding effects to enhance the catalytic reactivity of peptide-capped nanoparticles*. Journal of the American Chemical Society, 2013. **135**(30): p. 11048-11054.
45. Singh, S., et al., *Biologically programmed synthesis of core-shell CdSe/ZnS nanocrystals*. Chemical Communications, 2010. **46**(9): p. 1473-1475.
46. Johnson, A.K., et al., *Novel method for immobilization of enzymes to magnetic nanoparticles*. Journal of Nanoparticle Research, 2008. **10**(6): p. 1009-1025.
47. Abdelhamid, M.A., et al., *Affinity purification of recombinant proteins using a novel silica-binding peptide as a fusion tag*. Applied Microbiology and Biotechnology, 2014. **98**(12): p. 5677-5684.
48. Taniguchi, K., et al., *The Si-tag for immobilizing proteins on a silica surface*. Biotechnology and Bioengineering, 2007. **96**(6): p. 1023-1029.
49. Coyle, B.L. and F. Baneyx, *A cleavable silica-binding affinity tag for rapid and inexpensive protein purification*. Biotechnology and Bioengineering, 2014. **111**(10): p. 2019-2026.
50. Kacar, T., et al., *Directed self-immobilization of alkaline phosphatase on micro-patterned substrates via genetically fused metal-binding peptide*. Biotechnology and Bioengineering, 2009. **103**(4): p. 696-705.
51. Hnilova, M., et al., *Peptide-directed co-assembly of nanoprobe on multimaterial patterned solid surfaces*. Soft Matter, 2012. **8**(16): p. 4327-4334.
52. Verma, M.L., C.J. Barrow, and M. Puri, *Nanobiotechnology as a novel paradigm for enzyme immobilisation and stabilisation with potential applications in biodiesel production*. Applied Microbiology and Biotechnology, 2013. **97**(1): p. 23-39.
53. Buthe, A., S. Wu, and P. Wang, *Nanoporous silica glass for the immobilization of interactive enzyme systems*, in *Enzyme Stabilization and Immobilization*. 2011, Springer. p. 37-48.
54. Stine, K.J., K. Jefferson, and O.V. Shulga, *Nanoporous gold for enzyme immobilization*, in *Enzyme Stabilization and Immobilization*. 2011, Springer. p. 67-83.
55. Pierre, A., *The sol-gel encapsulation of enzymes*. Biocatalysis and Biotransformation, 2004. **22**(3): p. 145-170.
56. Zhang, Y.-H.P., et al., *Toward low-cost biomanufacturing through in vitro synthetic biology: bottom-up design*. Journal of Materials Chemistry, 2011. **21**(47): p. 18877-18886.
57. Ho, L.-F., et al., *Integrated enzyme purification and immobilization processes with immobilized metal affinity adsorbents*. Process Biochemistry, 2004. **39**(11): p. 1573-1581.
58. Nygaard, S., R. Wendelbo, and S. Brown, *Surface-specific zeolite-binding proteins*. Advanced Materials, 2002. **14**(24): p. 1853-1856.
59. Chen, N., *Hydrophobic properties of zeolites*. The Journal of Physical Chemistry, 1976. **80**(1): p. 60-64.
60. Ye, X., et al., *Synthetic metabolic engineering-a novel, simple technology for designing a chimeric metabolic pathway*. Microbial Cell Factories, 2012. **11**(1): p. 120.
61. Hodgman, C.E. and M.C. Jewett, *Cell-free synthetic biology: thinking outside the cell*. Metabolic Engineering, 2012. **14**(3): p. 261-269.
62. Swartz, J.R., *Transforming biochemical engineering with cell-free biology*. AIChE Journal, 2012. **58**(1): p. 5-13.
63. You, C. and Y.-H.P. Zhang, *Cell-free biosystems for biomanufacturing*, in *Future Trends in Biotechnology*. 2013, Springer. p. 89-119.
64. Rosales-Calderon, O., H.L. Trajano, and S.J. Duff, *Stability of commercial glucanase and  $\beta$ -glucosidase preparations under hydrolysis conditions*. PeerJ, 2014. **2**: p. e402.

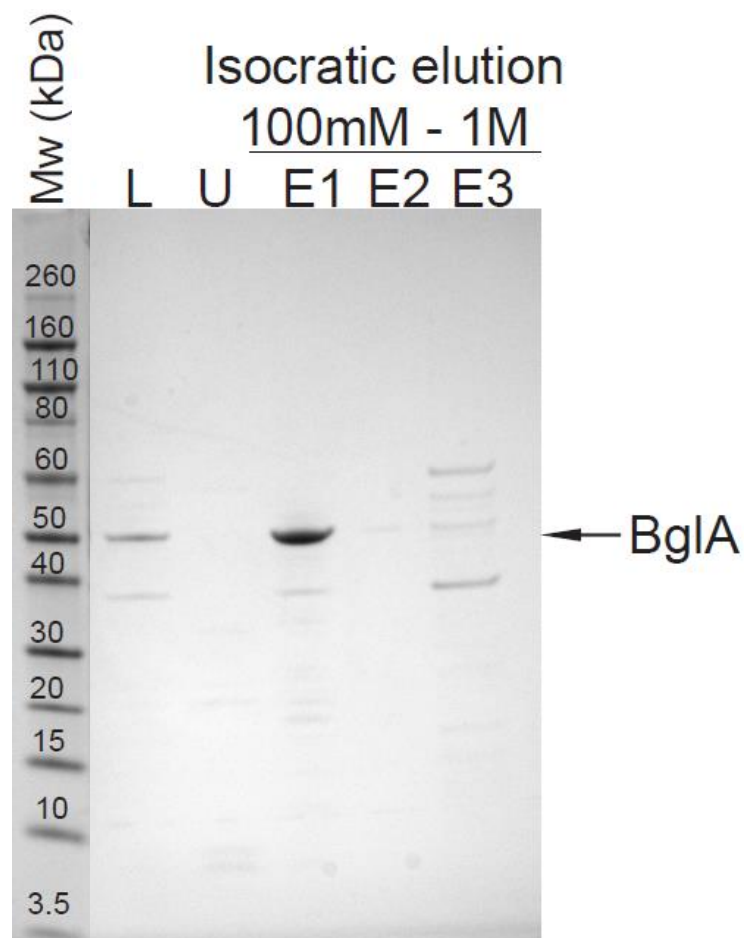
65. Morris, D.D., et al., *Cloning of the xynB Gene from Dictyoglomus thermophilum Rt46B. 1 and Action of the Gene Product on Kraft Pulp*. Applied and Environmental Microbiology, 1998. **64**(5): p. 1759-1765.
66. Bergquist, P., et al., *Genetics and potential biotechnological applications of thermophilic and extremely thermophilic microorganisms*. Biotechnology and Genetic Engineering Reviews, 1987. **5**(1): p. 199-244.
67. Gibbs, M.D., et al., *Sequencing and expression of a  $\beta$ -mannanase gene from the extreme thermophile Dictyoglomus thermophilum Rt46B. 1, and characteristics of the recombinant enzyme*. Current Microbiology, 1999. **39**(6): p. 351-357.
68. Love, D.R. and M.B. Streiff, *Molecular cloning of a  $\beta$ -glucosidase gene from an extremely thermophilic anaerobe in E. coli and B. subtilis*. Nature Biotechnology, 1987. **5**(4): p. 384-387.
69. Schauder, B., et al., *Inducible expression vectors incorporating the Escherichia coli atpE translational initiation region*. Gene, 1987. **52**(2): p. 279-283.
70. Bailey, M.J., P. Biely, and K. Poutanen, *Interlaboratory testing of methods for assay of xylanase activity*. Journal of Biotechnology, 1992. **23**(3): p. 257-270.
71. Britton, H.T.S. and R.A. Robinson, *CXCVIII.—Universal buffer solutions and the dissociation constant of veronal*. Journal of the Chemical Society (Resumed), 1931: p. 1456-1462.
72. Yu, H., et al., *Cross-linked enzyme aggregates (CLEAs) with controlled particles: application to Candida rugosa lipase*. Journal of Molecular Catalysis B: Enzymatic, 2006. **43**(1): p. 124-127.
73. Sangeetha, K. and T.E. Abraham, *Preparation and characterization of cross-linked enzyme aggregates (CLEA) of subtilisin for controlled release applications*. International Journal of Biological Macromolecules, 2008. **43**(3): p. 314-319.
74. Cui, J.D. and S.R. Jia, *Optimization protocols and improved strategies of cross-linked enzyme aggregates technology: current development and future challenges*. Critical Reviews in Biotechnology, 2013. **35**(1): p. 15-28.
75. Brady, D., et al., *Spherezymes: A novel structured self-immobilisation enzyme technology*. BMC Biotechnology, 2008. **8**(1): p. 8.
76. Lejeune, A., et al., *Quantitative analysis of the stabilization by substrate of Staphylococcus aureus PC1  $\beta$ -lactamase*. Chemistry & Biology, 2001. **8**(8): p. 831-842.
77. Schoevaart, R., et al., *Preparation, optimization, and structures of cross-linked enzyme aggregates (CLEAs)*. Biotechnology and Bioengineering, 2004. **87**(6): p. 754-762.
78. Pescador, P., et al., *Efficiency of a bienzyme sequential reaction system immobilized on polyelectrolyte multilayer-coated colloids*. Langmuir, 2008. **24**(24): p. 14108-14114.
79. Zhang, W., K. Lou, and G. Li, *Expression and characterization of the Dictyoglomus thermophilum Rt46B. 1 xylanase gene (xynB) in Bacillus subtilis*. Applied Biochemistry and Biotechnology, 2010. **160**(5): p. 1484-1495.
80. Hong, M.-R., et al., *Characterization of a recombinant  $\beta$ -glucosidase from the thermophilic bacterium Caldicellulosiruptor saccharolyticus*. Journal of Bioscience and Bioengineering, 2009. **108**(1): p. 36-40.
81. Larson, E.D., *A review of life-cycle analysis studies on liquid biofuel systems for the transport sector*. Energy for Sustainable Development, 2006. **10**(2): p. 109-126.
82. Carroll, A. and C. Somerville, *Cellulosic biofuels*. Annual Review of Plant Biology, 2009. **60**: p. 165-182.
83. Cho, E.J., et al., *Co-immobilization of three cellulases on Au-doped magnetic silica nanoparticles for the degradation of cellulose*. Chemical Communications, 2012. **48**(6): p. 886-888.
84. Tran, C.T., et al., *Celb and  $\beta$ -glucosidase immobilization for carboxymethyl cellulose hydrolysis*. RSC Advances, 2013. **3**(45): p. 23604-23611.
85. Hirsh, S., et al., *Linker-free covalent thermophilic  $\beta$ -glucosidase functionalized polymeric surfaces*. Journal of Materials Chemistry, 2011. **21**(44): p. 17832-17841.

86. Nosworthy, N.J., et al., *Ion implantation treatment of beads for covalent binding of molecules: Application to bioethanol production using thermophilic beta-glucosidase*. Enzyme and Microbial Technology, 2014. **54**: p. 20-24.

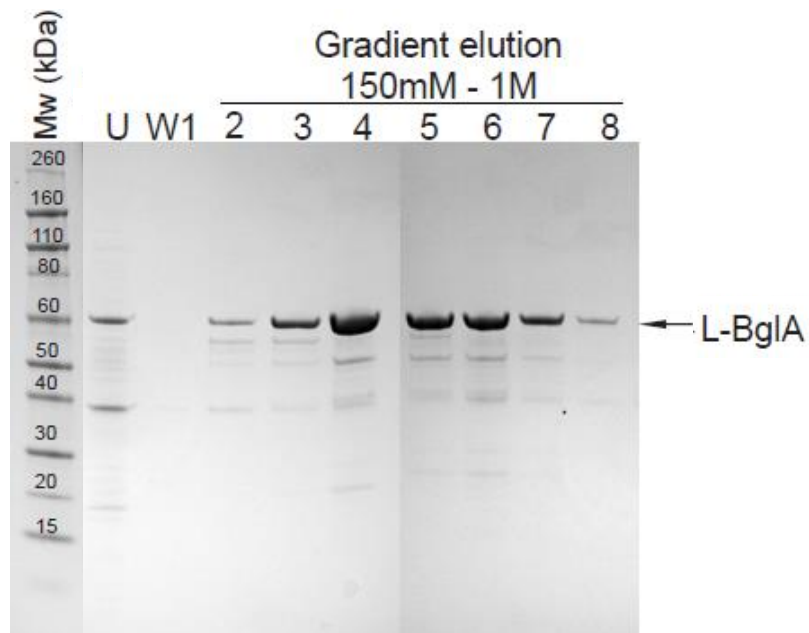


## Chapter 6 Supplementary material

Ion-exchange chromatography was attempted to purify samples of BglA and L-BglA, but was ultimately unsuccessful. The methodology and results are presented here in the supplementary material section.



Chromatographic purification of BglA using a Hi-Trap Q HP column (5mL, GE Healthcare Life Sciences). BglA eluted at the 100mM NaCl wash step, and other cellular proteins remained bound to the column until the 1M wash. L; supernatant of heat-denatured soluble fraction that was loaded into the Q column, U; unbound flowthrough from sample load, E1; elution fraction from 100mM NaCl column wash (contains BglA), E2; elution fraction from 200mM NaCl column wash, E3; elution fraction from 1M NaCl wash.



Chromatographic purification of L-BglA using a Hi-Trap SP HP column (5mL, GE Healthcare Life Sciences). Fractions 2-8 eluted at approximately 0.3M NaCl over a gradient from 0.15-1M. Fractions 3-8 were combined and used for further data collection.

L; supernatant of heat-denatured soluble fraction that was loaded into the SP column, U; unbound flowthrough from sample load, W1; 150mM NaCl column wash, 2-8; NaCl gradient elution fractions, at approx. 300mM NaCl (contains L-BglA).